MINISTRY OF EDUCATION AND RESEARCH
National University of Science and Technology
POLITEHNICA Bucharest
Doctoral School of Industrial Engineering

LAZĂR M. Marius-Vali

PhD THESIS

Abstract

Contributions to the modeling and precision evaluation of elements and molds made of thermoplastic materials produced by additive manufacturing and cutting

***PhD Scientific Adviser*,**
Prof.univ.dr.ing. Marian GHEORGHE

- 2026 -

Foreword

The research and contribution to the modeling and evaluation of the precision of thermoplastic molds produced by additive manufacturing and cutting represent the *motivation* and *direction* of the doctoral studies, completed by this doctoral thesis. It represents the result of a particularly challenging, but also rewarding, professional and academic journey.

The doctoral program consisted of preparing, presenting and taking exams and scientific reports, determining and analyzing roughness functions and dimension functions, developing numerical models for simulating manufacturing processes, proposing and developing thermoplastic molds, producing and publishing scientific papers, and developing this doctoral thesis on modeling and evaluating the accuracy of thermoplastic molds produced by additive manufacturing and machining.

In the completion of this work, an important role was played by the doctoral adviser, Mr. Prof. univ. dr. eng Marian GHEORGHE, to whom I express my sincere thanks for the guidance, trust and all the support provided during the doctoral studies.

I would like to express my sincere gratitude to Prof. Dr. Eng. Cristian DOICIN, Prof. Dr. Eng. Sergiu TONOIU, Assoc. Prof. Dr. Eng. Cătălin GHEORGHIȚĂ, Assoc. Prof. Dr. Eng. Ovidiu BLĂJINĂ from the Department of Machine Construction Technology, POLITEHNICA Bucharest, as well as to Prof. Dr. Eng. Oana DODUN from the "Gheorghe Asachi" Technical University of Iași, for the constructive comments and recommendations given during doctoral studies, as well as within the Committee of academic guidance and integrity.

I would like to thank Prof. Dr. Eng. Nicolae IONESCU from the National University of Science and Technology POLITEHNICA Bucharest. Prof. Dr. Eng. Laurențiu SLĂTINEANU and Prof. Dr. Eng. Gheorghe NAGÎȚ from the Technical University "Gheorghe Asachi" of Iași, Prof. Dr. Eng. Tom SAVU from the National University of Science and Technology POLITEHNICA Bucharest for the comments and recommendations made within the Committee for the evaluation and public defense of the doctoral thesis.

I would also like to express my gratitude to all my colleagues from the TCM Department for their support, especially to Mr. Lec. dr. eng. Bogdan JUGRAVU and Mrs. Lec. dr .eng. Manuela DIJMĂRESCU.

I express my profound gratitude to the Faculty and Department leadership to which I belong, especially to Mr. Prof. univ. dr. ing. Tom SAVU, who gave me the chance and freedom to develop myself and pass on the knowledge acquired over the years of study.

I would like to express my gratitude to Mr. Lec. dr. eng. Tudor George ALEXANDRU and Mr. Lec. dr. eng. Constantin STOCHIOIU for all their support.

I would like to express my special thanks to my girlfriend, Silvia, for her support, patience and understanding throughout the writing of this thesis. Her constant encouragement and support have been a source of encouragement and balance for me.

I would like to thank my family for all the support they have given me, without them, my path in life would have been much more difficult.

Marius-Vali LAZĂR

Introduction

Products made of polylactide, PLA, or glycol-modified polyethylene terephthalate, PETG, as well as other categories of thermoplastic materials can be manufactured by 3D printing, casting, injection molding, extrusion, machining, etc., as appropriate. In individual or small-scale production, PLA and PETG can be used in industry to manufacture molds, by 3D printing, for injection molding, cold bending, etc

The research and development activity within the doctoral program aims to model and evaluate the precision of elements and molds made of thermoplastic materials produced by additive manufacturing and machining, with a focus on the thermoplastic polymer materials PLA and PETG.

* * *

In the first part of the doctoral thesis, based on the analysis of the current state of research on the manufacturing and precision of elements and molds made of thermoplastic materials produced by additive manufacturing and machining, relevant data are presented regarding: the development of molds made of resin, polyjet, polyetheretherketone, polylactide and other polymeric materials; the development of molds made of thermoplastic materials for bending processing; main categories of machining; elements regarding the mechanics of the machining process; research on the machining of elements made of thermoplastic materials; conclusions.

In the second part of the doctoral thesis, based on the data and conclusions drawn from the analysis of the current state, research and development directions are presented and the main objective of the advanced doctoral research and development activity is determined as: modeling and evaluating the accuracy of elements and molds made of thermoplastic materials produced by additive manufacturing and machining. The research and development methodology is also presented.

Next, complex, high-volume theoretical and experimental research is initiated, developed and carried out on: the roughness and dimensional accuracy of 3D printed PLA parts processed by CNC milling; the roughness and dimensional accuracy of 3D printed PETG parts processed by CNC milling; the development of technological models in PLA for the manufacture of silicone molds applied to the casting of polyurethane resin parts; finite element analysis, manufacturing and testing of cold bending molds in PLA and PETG.

In the last part of the doctoral thesis, the general conclusions and the main contributions made by the doctoral thesis to the modeling and evaluation of the precision of elements and molds made of thermoplastic materials produced by additive manufacturing and machining are presented, the scientific importance of the doctoral thesis, the practical importance of the doctoral thesis, as well as perspectives of the development of products made of thermoplastic materials through assisted design, additive manufacturing and CNC machining, as potential future directions, through continuous, complex and profound research and development activity.

Legend

01	A_0	Initial cross-sectional area
02	ABS	Acrylonitrile butadiene styrene
03	a_p	Depth of cut
04	B	Width
05	B_0	Initial width
06	B_i	Current width
07	C	Objective dimension
08	CAD	Computer Aided Design
09	CNC	Computerized Numerical Control
10	DIC	Digital imagine correlation
11	e	Radial feed increment
12	E	Modulus of elasticity
13	EE	Experimental error
14	f	Feed
15	F	Feed rate
16	FC	Cylindrical milling
17	FC-F	Cylindrical-face milling
18	FDM	Fused deposition modeling
19	FEA	Finite element analysis
20	FEM	Finite element method
21	F_f	Feed force
22	FF	Face milling
23	F_i	Current traction force
24	f_z	Feed per tooth
25	g	Thickness
26	IPA	Isopropyl alcohol
27	L_0	Initial length
28	L_i	Current length
29	MIV	V bending die
30	MS	Silicone mold
31	MSMIV	Structural model of V bending die

32	MT	Technological model
33	n_c	Spindle speed / Rotational speed
34	p	Axial feed increment
35	P	Product
36	PA	Piece A
37	PB	Piece B
38	PDMS	Polydimethylsiloxane
39	PEEK	Polyether ether ketone
40	PETG	Polyethylene terephthalate glycol
41	Pg	Piece with thickness g
42	PLA	Polylactic acid
43	PMEE	Mean square of experimental errors
44	PMB	Mean square of regression
45	PMI	Mean square of lack-of-fit
46	PMMA	Polymethyl methacrylate
47	PMRZ	Mean square of residuals
48	PMSA	Hydrogel
49	PVB	Polyvinyl butyral
50	R	Fillet radius
51	R^2	Coefficient of determination
52	SI	Inclined surfaces
53	SO	Horizontal surfaces
54	SV	Vertical surfaces
55	SLA	Stereolithography
56	SPB	Sum of squares due to regression
57	SPEE	Sum of squares of experimental errors
58	SPI	Sum of squares of lack-of-fit
59	SPRZ	Sum of squares of residuals
60	V_c	Cutting speed
61	ΔL	Current elongation
62	ν	Poisson's ratio

Chapter 1. Research on the development of molds from polymeric materials produced by additive manufacturing

In individual or small-scale production conditions, components of injection or casting molds can be designed and produced through additive manufacturing from polymeric materials such as resin, polylactic acid, etc. [1 - 11].

1.1. Development of resin molds, polyjet RGD515 and polyetheretherketone

Elements regarding 3D printing of active plates from the construction of an injection mold, in different technological variants [24], are as presented in Table 1.1.

Tabelul 1.1. Elements regarding 3D printing of active plates in the construction of an injection mold (adapted from [24])

Printing technology	Printer 3D	Material printat
Stereolithography (SLA)	Formlabs Form 2	Formlabs White Resin
Polyjet	Stratasys Polyjet Object 350	Polyjet Object RGD515
Fused Deposition Modeling (FDM)	Intamsys Funmat HT	Polieter ether ketone (PEEK)

1.2. Development of molds made of polylactide and other polymeric materials

Polylactide or polylactic acid, PLA, is a thermoplastic polymer material that is produced in a wide range of chemical and physical characteristics, respectively, with a density of 1.21 – 1.43 kg/dm3, a melting point of 150 -160 °C, an elastic modulus of 2.7 – 16 GPa, etc. [91].

PLA products can be manufactured by 3D printing, casting, injection molding, extrusion, mechanical processing, etc. [91, 92, 93].

Due to its low cost, polylactide (polylactic acid), PLA, is a material used in industry for the manufacture of 3D printing molds - in the case of small or one-off series production, in the field of injection molding, etc. [12 - 23].

PLA can be used in molds in which natural composite elements are formed. This technology is developing under the conditions of the circular economy. Three hybrid molds printed from PLA and, respectively, silicone (Fig. 1.3) were used to cast natural "green" composites in the combination of: fir resin, wax, fir needles, ground fir needles, rice, ground rice, quisetum and ground quisetum, in the form of specific specimens for mechanical tests in bending, impact and compression [25].

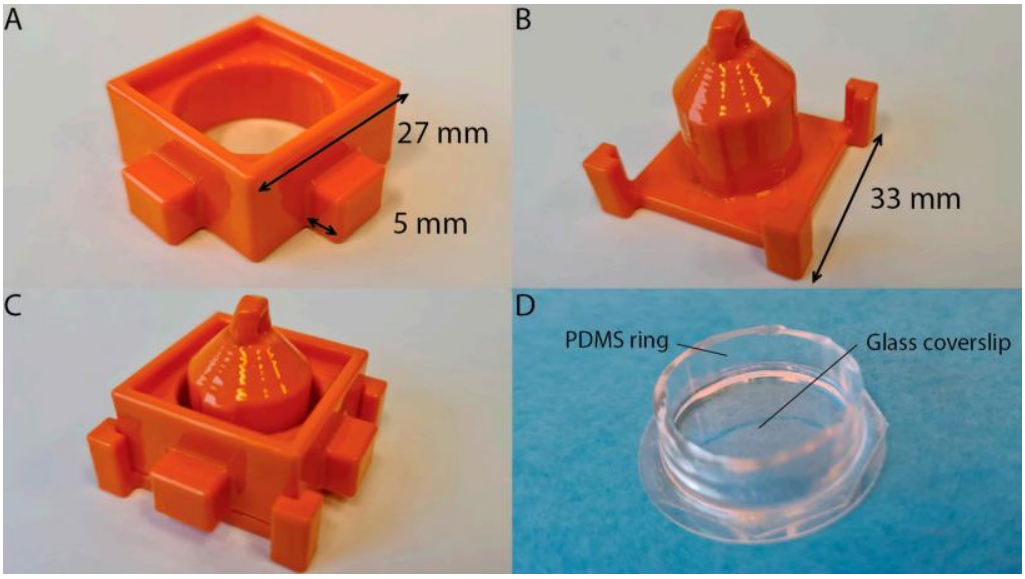


Fig. 1.4. 3D printed mold made of PLA and the part produced from PDMS [26]

Tan E.T.W. et al. used 3D printed elements from PLA to obtain an acrylic bone cement implant. Thus, by scanning, a 3D model of a skull was made, the mold on which the cement is molded after obtaining the cranial implant was designed and 3D printed from PLA (Fig. 1.11) [32].

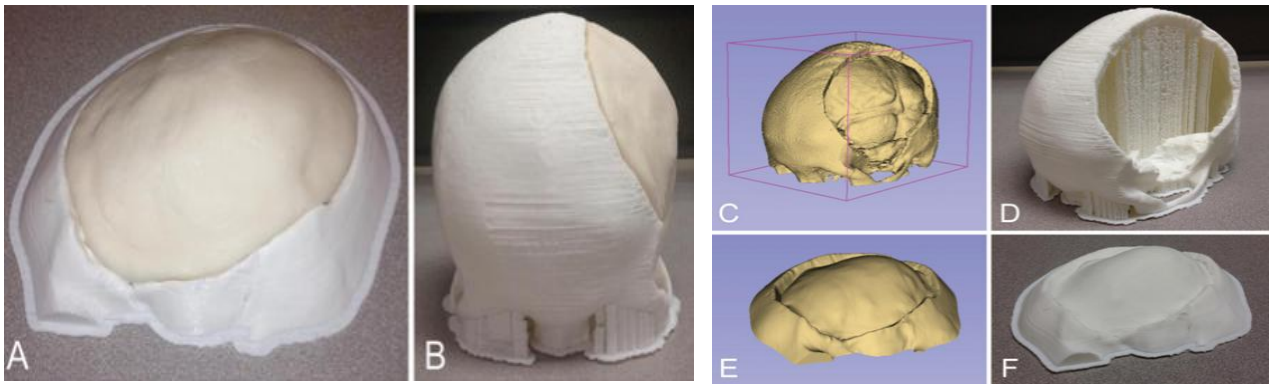


Fig. 1.11. 3D printed elements and bone cement: A) acrylic bone cement on the mold; B) implant mounted on the 3D printed skull; C) 3D model of the skull; D) printed skull; E) 3D model of the mold; F) printed mold [32]

What is different about this method is the way in which the symmetry of the skull is checked. For this, a 3D PLA skull was printed showing the location of the implant. After obtaining the implant, it is mounted on the printed skull, which is then 3D scanned, and the degree of symmetry is determined using a computer [32].

1.3. Development of thermoplastic molds for cold bending processing

Nakamura et al. evaluated the deformations occurring during V-bending using the digital image correlation (DIC) method. The dimensions of the dies are shown in Fig. 1.18 [105].

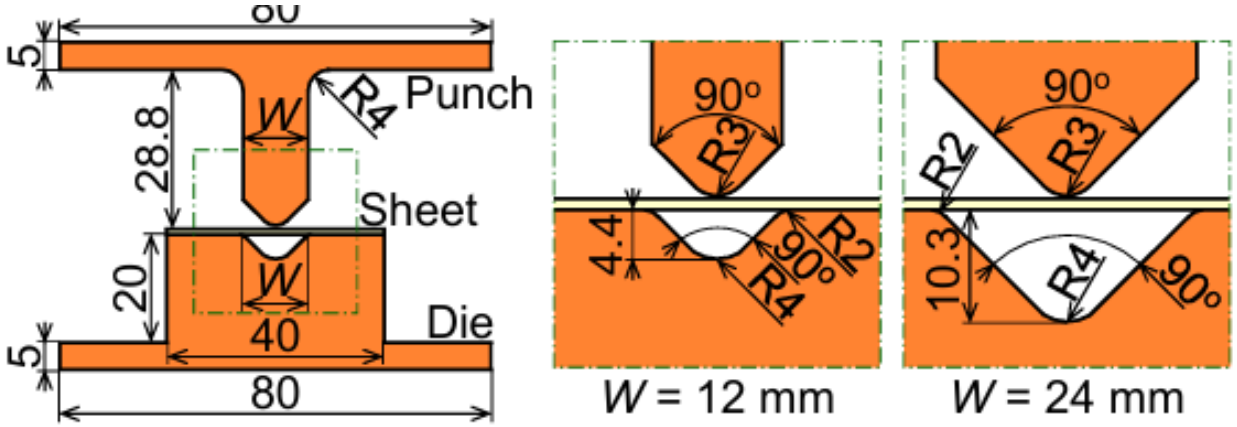


Fig. 1.18. Dimensions of V-bending dies [105]

The molds were manufactured from PLA on a FLASHFORGE INVENTOR 3D printer, and the printing parameters used were: nozzle temperature – 200 °C, bed temperature - 50 °C, layer thickness – 0.18 mm, filling degree of 80%. Young's modulus (2900 MPa) and Poisson's ratio (0.33) were determined using the DIC method [105].

In order to avoid friction problems, the mold elements were manually finished with an abrasive paper. Using the DIC method, some deformation maps were observed during the bending process (Fig. 1.20.) [105].

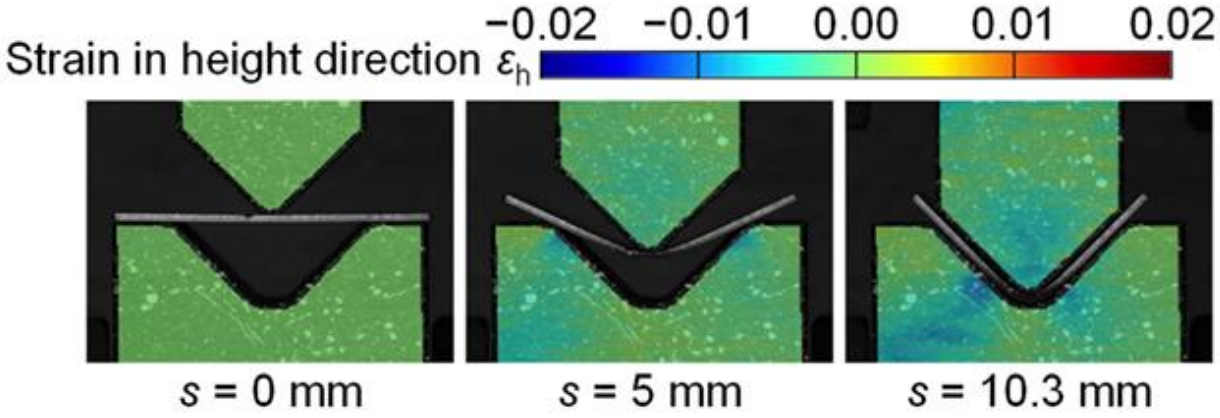


Fig. 1.20. Example of a deformation map, bending steel with a tensile strength of 980 MPa, punch width W: 24 mm [105]

Higher forces occur in the case of bending with a smaller punch width (W=12 mm) (Fig. 1.21), and the maximum deformations occur in the connection area [105].

Chapter 2. Research on machining of thermoplastic products

Products made of polylactide, PLA, or glycol-modified polyethylene terephthalate, PETG, as well as other categories of thermoplastic materials can be manufactured by 3D printing, casting, injection molding, extrusion, mechanical processing, etc., as appropriate [91- 93, 97 - 100].

2.1. Main categories of machining operations

There are various categories of machining processes – turning, drilling, milling, etc., which can be applied to thermoplastic semi-finished products/parts, each of which has a series of specific technical and economic characteristics.

2.2. Elements regarding the mechanics of the cutting process

Geometric and kinematic characterization

In metal cutting theory, all machining operations performed with wedge-shaped tools, resulting in metal removal in the form of chips, can be conventionally divided into two general cases, orthogonal cutting and oblique cutting, respectively [50], as shown in Fig. 2.8.
The wedge-shaped tool geometry essentially leads to the intersection of two surfaces to form the straight cutting edge. Functionally, the surface on which the chip slides is called the clearance surface, and the surface that is in contact with the workpiece is the seating surface.

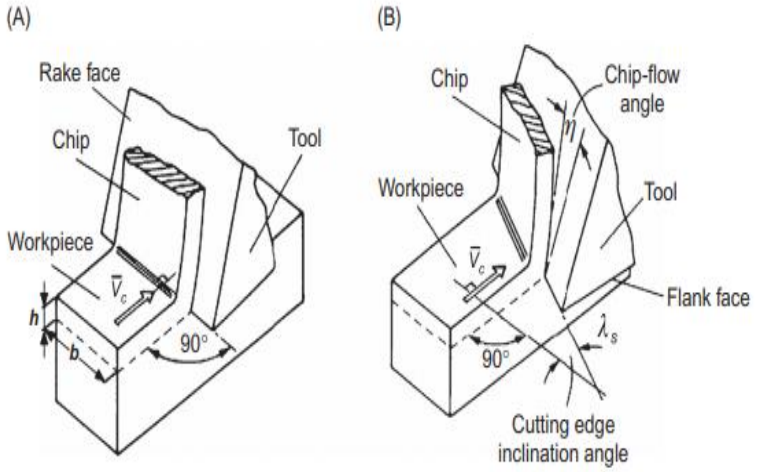


Fig. 2.8. A) Orthogonal cutting, B) Oblique cutting [51, 52]

Orthogonal cutting is more of a 2D problem, leading to a simple cutting process that is often used in research [50]. It allows the adoption of a process model that incorporates the plastic deformations and cutting stresses in the cutting zone of the material. The vectors of tool motion, deformed material slip and chip velocity for orthogonal and oblique cutting are represented in Fig. 2.9 [50].

2.3. Research on the machining of thermoplastic elements

Products made of polylactide (polylactic acid), PLA, can be manufactured by 3D printing, casting, injection molding, extrusion, machining, etc. [91, 92, 93].

Additive manufacturing is a method often used in prototyping, which allows complex geometries to be achieved with low energy consumption. Despite these advantages, the method has not yet been implemented in mass production, due to low repeatability and process stability [57 - 62].

In some areas of industry, parts made of polylactide, PLA, are required, which require low roughness and high dimensional accuracy. A finishing process is necessary to remedy these deficiencies [63 - 65]. To improve the roughness, there are methods based on the use of acetone-based substances [66] or isopropyl alcohol, which, however, do not lead to high dimensional accuracy [28]. Other methods need to be developed to achieve both good roughness and high dimensional accuracy. One of the methods is machining on classical machine tools or on numerically controlled machine tools [67].

Mehtedi M.E. et al. investigate the machinability of 3D printed PLA parts by milling [68]. Thus, they conducted an experiment on the influence of feed rate, depth of cut and speed on roughness and burr during milling. For 3D printing, they chose FDM technology, using PLA (PLA LITE – 4043D) from NatureWorks LLC. The mechanical properties provided by the manufacturer are presented in Table 2.1. The 3D printing machine used was TRONXY 5SA FMD. A cleaning spray was applied to avoid problems with parts detaching from the machine table [68].

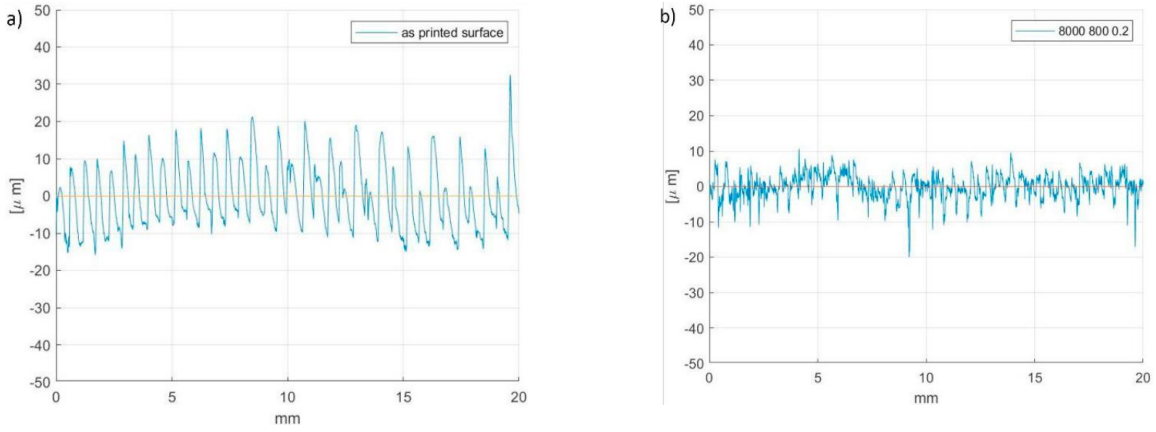


Fig. 2.12. Comparison of the roughness parameters Ra resulting from: a) 3D printing; b) milling [68]

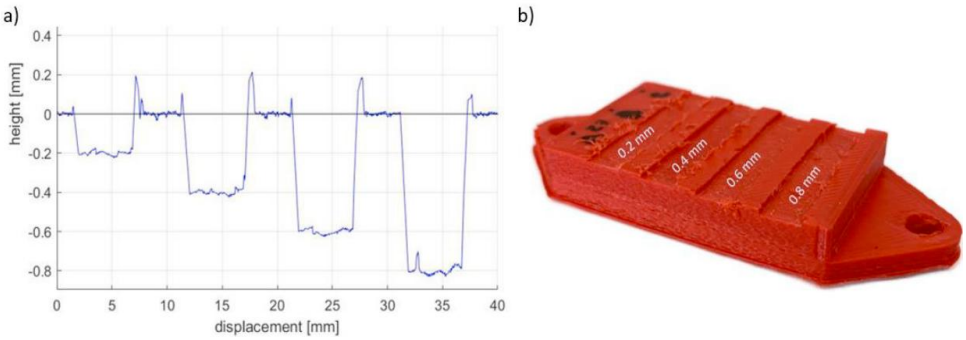


Fig. 2.13. a) Profile perpendicular to the machining direction; b) part after machining [68]

Graphs of dependence between roughness Ra and cutting parameters are presented (Fig. 2.14-a), as well as between burr height and cutting parameters (Fig. 2.14-b) [68].

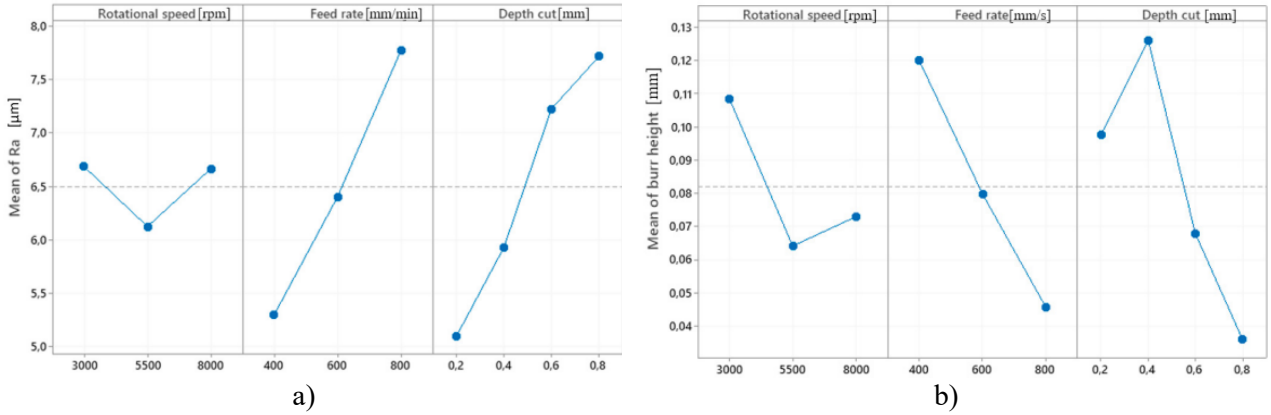


Fig. 2.14. Dependence graphs between: a) Ra and nc, Vf, ap; b) burr height and nc, Vf, ap [68]

Chapter 3. Conclusions regarding the state of art on manufacturing and precision of thermoplastic elements and molds produced by additive manufacturing and machining

From the analysis of the current state of research on the manufacturing and precision of thermoplastic elements and molds produced by additive manufacturing and machining, important conclusions can be drawn, as follows.

• In individual or small-scale production conditions, components of injection or casting molds can be designed and produced by additive manufacturing from polymer materials such as resin, polylactic acid, etc.

Experimental research on the additive manufacturing of active plates in the construction of an injection mold, in different technological variants, respectively, from various materials - white resin, polyetheretherketone, polyjet RGD515 -, showed that the dimensional precision of the manufactured elements - for example, polylactic acid (PLA) pellets - is acceptable (see § 1.1).

• Polylactide (PLA) is a thermoplastic polymer material that is produced in a wide range of chemical and physical characteristics, respectively, with a density of 1.21 – 1.43 kg/ dm^3, an elastic modulus of 2.7 – 16 GPa, etc. (see § 1.2).

• PLA products can be manufactured by 3D printing, casting, injection, extrusion, machining, etc. Due to its low cost, PLA is a material used in industry to manufacture 3D printed molds - in the case of small or unique series production, by injection molding, etc. (see § 1.2).

• 3D printed molds are an acceptable option due to their low price, but a main problem is the roughness of the mold surfaces.

PLA molds are a more economical and faster solution than resin molds, which require special printing machines, to manufacture parts from polydimethylsiloxane. (PDMS) (see § 1.2).

• Mold finishing with chloroform vapor provides good roughness but low dimensional accuracy. 3D printed mold finishing can be done by manual sandblasting for components with simple geometry and high tolerances. (see § 1.2).

• In a research, a method was developed to obtain silicone prostheses using 3D printed molds finished with acetone (see § 1.2).

• One method of obtaining implants from acrylic bone cement is to cast the base material over a 3D printed mold (see § 1.2).

• Silicone molds can be used for the manufacture of PMMA implants. To model the active parts of the molds, 3D printed technological models made of PLA are frequently used. This method can be applied on a large scale, being cheap and with good results (see § 1.2).

A silicone mold generally requires a low volume of surface preparation activities, since most materials do not adhere to silicone (see § 1.2).

• Research on the bending of V-shaped parts using 3D printed PLA molds focuses on the deformations of the active elements and the forces during the process. It is shown that the maximum deformation values were measured when bending the part made of the material with a tensile strength of 980 MPa (approximately -0.02 mm) (see § 1.3).

• Products made of polylactide, PLA, or glycol-modified polyethylene terephthalate, PETG, as well as other categories of thermoplastic materials can be manufactured by 3D printing, casting, mechanical processing, etc.

There are various categories of machining processes – turning, drilling, milling, etc., which can be applied to thermoplastic semi-finished products/parts, each of which has a series of specific technical and economic characteristics (see § 2.1).

• Research into the machinability of 3D printed parts made of PLA, within an experimental program, based on a three-factor factorial design, aimed at the influence of cutting depth, feed and cutting speed on roughness and burr during milling processing with coolant. It is shown that the main parameter influencing roughness is the feed per tooth (see § 2.3).

• A research on the processing of parts using the hybrid method, namely 3D printing and CNC milling, in which the thickness of the deposition layer is varied, highlights the fact that the most uniform surface was achieved with the smallest layer thickness.

One of the main advantages of using this hybrid solution is the elimination of orientation errors, since both processes (printing and CNC milling) are performed in the same position in the machine workspace. An 80% improvement in accuracy was achieved by milling (see § 2.3).

• In the research focusing on the milling machinability of 3D printed parts made of PLA, PETG and CF-PETG, an experiment is designed to analyze the influences of feed rate, depth of cut and speed on milling roughness and burr. Graphs of dependence between cutting parameters and roughness/ burr height are presented. (see § 2.3).

• In an experimental research on the milling machinability of 3D printed parts made of PETG and CF-PETG, the influence of the orientation of the semi-finished products relative to the printing direction and the thickness of the deposited layer on the roughness and effective dimensions is studied.

In the case of milling PETG parts, the effective values of roughness and dimensional accuracy are not influenced by the way the parts were previously manufactured (orientation relative to the printing direction or the thickness of the deposited layer). In the processing of CF-PETG parts, the influence of obtaining the semi-finished products on the effective values is highlighted (see § 2.3).

• Research on hybrid manufacturing (3D printing + machining) of 3D printed parts from PETG aims at the influence of some machining parameters and the thickness of the deposited layer on the effective roughness. In the experiments, the parts are turned using a carbide tipped cutter with a radius at the tip. It is highlighted how the feed rate influences the effective roughness (see § 2.3)

Chapter 4. The directions, main objective and methodology of research and development regarding the modeling and precision evaluation of elements and molds made of thermoplastic materials produced by additive manufacturing and cutting

4.1. Research and development directions

Based on the analysis of the current state, the following research and development directions are considered promising for the development of thermoplastic elements and molds:

• determining the material and geometric characteristics of thermoplastic elements and molds;

• interaction processes between the characteristics of thermoplastic molds and elements of technological systems;

• constructive - functional databases regarding thermoplastic elements and molds;

• processes and systems for manufacturing thermoplastic elements and molds;

• technological databases regarding thermoplastic elements and molds;

• case studies regarding the design and manufacture of thermoplastic elements and molds.

4.2. The main objective of the research and development activity

Considering the data and conclusions drawn from the analysis of the current state, as well as the research and development directions regarding the development of elements and molds made of thermoplastic materials, the main objective of the advanced doctoral research and development activity is determined as**: modeling and precision evaluation of elements and molds made of thermoplastic materials produced by additive manufacturing and cutting.**

4.3. Research and development methodology

The research and development methodology is designed as a set of reference elements for achieving the main objective of the doctoral thesis and, accordingly, the theoretical and experimental research program, respectively, the specific chapters of the doctoral thesis, as well as future developments.

The theoretical and experimental research program is structured as shown in Fig. 4.1.

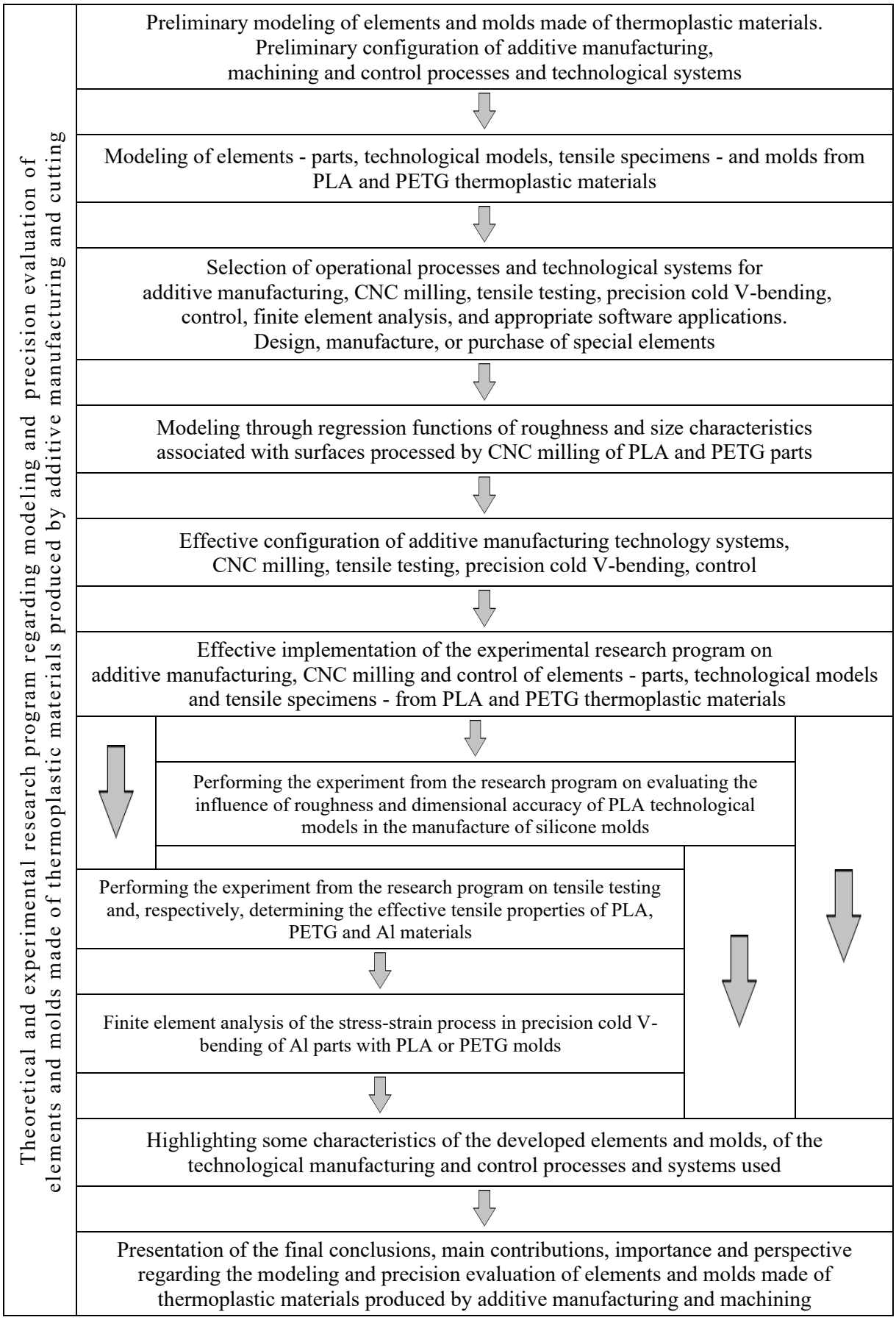


Fig. 4.1. General structure of the theoretical-experimental research program

Chapter 5. Research on the roughness and dimensional precision of 3D printed PLA parts processed by CNC milling

Research on the roughness and dimensional precision of 3D printed PLA parts processed by CNC milling, which also includes published elements of the author [74], is as follows.

5.1. Characteristics of research processes and systems for determining roughness and dimensional precision of 3D printed PLA parts processed by CNC milling

5.1.1. Research programs, PLA material, types of parts and surfaces, milling processing schemes, elements of 3D printing and CNC machining processes and technological systems

a. General elements regarding the PLA - Face Milling, PLA - Cylindrical Milling and PLA - Cylindrical-face Milling research programs

Considering the shape and relative position of the surfaces in the structure of some 3D printed PLA mold components (see also § 1.2, 2.3), as well as the different milling processing schemes

(see also § 2.1, 2.2), the PLA - Face Milling, PLA - Cylindrical Milling and PLA - Cylindrical-Face Milling research programs were developed through which, under defined conditions:

• a series of parts are 3D printed from PLA;

• for the printed parts, flat surfaces of different positions are processed by CNC milling, namely, *horizontal* flat surfaces - by face milling, *vertical* flat surfaces - by cylindrical milling, respectively, *inclined* flat surfaces - by cylindrical-face milling, as the case may be;

• the roughness parameters Ra and Rz are modeled and analyzed, as well as the dimensional accuracy related to some flat surfaces of the printed parts and, accordingly, related to the *horizontal, vertical, inclined* flat surfaces processed by CNC milling.

h. Objective surfaces and milling processing schemes

In order to evaluate the roughness and dimensional accuracy of CNC milling surfaces of 3D printed PLA parts, of type PA and PB (see Fig. 5.1), the target flat surfaces and target dimensions, as well as the milling processing schemes, were selected, as shown in Fig. 5.9, respectively: a *horizontal* flat surface - by face milling (PA/ SO - FF); two *vertical* flat surfaces and the dimension C of the distance between the two vertical flat surfaces - by cylindrical milling (PA/ SV1, 2; C – FC); an *inclined* flat surface - by cylindrical-face milling (PB/ SI – FC-F).

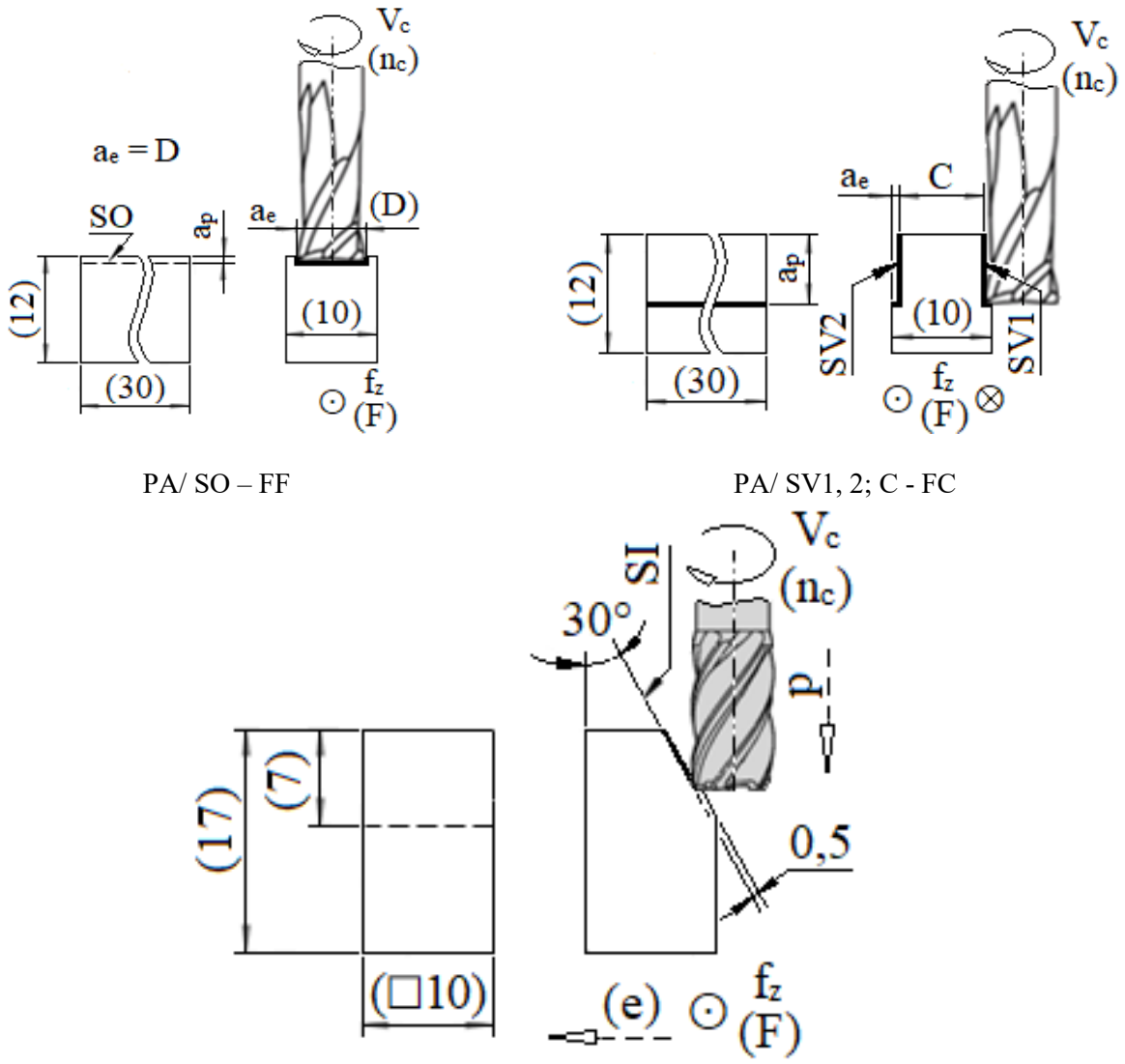


Fig. 5.9. Objective plane surfaces, objective dimension and machining schemes: *horizontal* surface - face milling (PA/ SO - FF); *vertical* surfaces and the distance between them - cylindrical milling (PA/ SV1, 2; C - FC); *inclined* surface - cylindrical-face milling (PB/ SI – FCF)

5.1.2. Evaluation of roughness and dimensional precision of 3D printed PLA parts

For a series of 3D printed parts made of PLA material, the effective roughness parameters, Ra* and Rz* of horizontal (frontal), vertical (lateral) and inclined surfaces, as well as the effective distance, C*, between two vertical (plane, parallel) surfaces were determined (see also Fig. 5.1 - PA, PB and § 5.1.1 - g, j, k). The results are presented in the Annex no. 1.1, and the average effective values - in Tables 5.5 and 5.6.

The following are noted (see also Tables 5.5, 5.6, Annex no. 1.1):

• for *horizontal* surfaces, the roughness parameter Ra* has effective values in the roughness classes

N 8 - 9 (Ra 3.2 - 6.3), and for *vertical* and *inclined* surfaces, the parameter Ra* has effective values in the roughness classes N10 - 11 (Ra 12.5 - 25) [94];

• the dimension C* has effective values in the tolerance class IT12 [95].

5.1.3. Elements of modeling the roughness and size associated with surfaces processed by face, cylindrical and cylindrical-face milling, in 3D printed parts made of PLA material

a. Process variables

In the modeling of the roughness and dimension associated with surfaces machined by end milling, cylindrical and cylindrical-end milling, for 3D printed parts made of PLA, the dependent and independent variables were selected, respectively,

• dependent variables: roughness parameters Ra and Rz, in μm, in the PLA - End/Cylindrical/End Milling programs, as well as the distance C, in mm, between two parallel surfaces machined in the PLA - Cylindrical Milling program;

• independent variables: feed per tooth, fz, and cutting speed, Vc, in the PLA - Cylindrical Milling program or the speed, n_c, and feed rate, F, in the PLA - End Milling program, as well as the axial adjustment feed, p, in the PLA - End Milling program.

Table 5.7. Elements regarding the parameters of cutting regimes (see also Tables 5.2 – 5.4, Fig. 5.4, 5.5, 5.9)

Processing	End mills T01, T02 of: active diameter d (D - at T01, D1 - at T02) and tip radius r (at T02), mm; number of teeth z				Depths of cut - axial (main), a_p, and radial (secondary), a_e, mm; Machining allowance, A, mm			Cutting feed, fz, mm/tooth; Cutting speed, Vc, m/min; Speed, n_c, rpm; Feed rate, F, mm/min; Adjustment feeds - axial, p, and radial, e, mm/pass					Number of passes
	Cod	d	r	z	a_p	a_e	A	f_z	V_c	n_c	F	p, e	i
Face milling	T 01	8		2	0,3	8		$f_z \in (0{,}012; 0{,}24)$, $V_c \in (55; 102)$, $n_c = 1000V_c/\pi d$, $F = zf_z n_c$, $n_c \in (2188; 4058)$, $F \in (52; 1210)$				-	1
Cylindrical milling					7	0,3						-	1
Cylindrical - face milling	T 02	8	0,5	5	p	A/cos 30°, $a_e = 0{,}58$	0,5					$p \in (0{,}008; 0{,}11)$, e = p*tg30°; i = (7 + r)/p, i = 7,5/p	

Next, the independent variables and each dependent variable are denoted by Xj, j = 1, 2, and Y, respectively,

$$X_1 = f_z,\ X_2 = V_c \text{ or } X_1 = F,\ X_2 = n \text{ or } X_1 = p,\ Y = Ra, Rz \text{ or } C, \text{ as appropriate} \quad (5.1)$$

b. Analytical models for regression functions of roughness and dimension of machined surfaces

Based on the results of theoretical and experimental research [74, 83], the analytical models for the roughness and dimension regression functions of machined surfaces were chosen, as follows.

(b1) Within the PLA programs - Face milling/Cylindrical milling, for the roughness and dimension regression functions of machined surfaces, respectively, the analytical model (multivariable) is chosen:

$$Y = A_0 X_1^{A_1} X_2^{A_2},\ X_1 = f_z,\ X_2 = V_c \text{ or } X_1 = F,\ X_2 = n_c,\ Y = Ra, Rz \text{ or } C, \text{ as appropriate} \quad (5.2)$$

Where A_0, A_1 și A_2 are the regression coefficients to be determined.

In order to determine the regression coefficients, the function $Y = A_0 X_1^{A_1} X_2^{A_2}$ is logarithmized, so that it becomes linear in relation to the regression coefficients, respectively,

$$\ln Y = \ln A_0 + A_1 \ln X_1 + A_2 \ln X_2,\ X_1 = f_z,\ X_2 = V_c \text{ or } X_1 = F,\ X_2 = n_c \text{ and } Y = Ra, Rz, C \quad (5.3)$$

or, equivalent,

$$y = a_0 + \sum_{j=1}^{2} a_j z_j,\ y = \ln Y,\ z_j = \ln X_J,\ a_0 = \ln A_0 \text{ și } a_J = A_J, j = 1, 2 \quad (5.4)$$

For dimensional homogenization, the dimensionless independent computational variables x_j are introduced, through the substitutions:

$$z_j = p_j x_j + q_j,\ j = 1, 2 \quad (5.5)$$

where the constants p_j and q_j are determined for corresponding levels of the variables z_j (X_j) și x_j.

Thus, the function (5.4) becomes:

$$y = b_0 + \sum_{j=1}^{2} b_j x_j,\ y = \ln Y,\ Y = Ra, Rz \text{ or } C, \text{ as appropriate} \quad (5.6)$$

where b_0 and b_j, j = 1, 2, are the regression coefficients that can be subjected to regression analysis in order to assess their significance and the adequacy of the model.

(b2) Within the PLA program - Cylindrical-face milling, for the machined surface roughness regression functions the analytical model (monovariable) is chosen:

$$Y = A_0 X_1^{A_1},\ X_1 = p,\ Y = Ra \text{ or } Rz \quad (5.7)$$

where A_0 and A_1 are the regression coefficients to be determined.

In the experimental data processing stage, using the Microsoft Excel application [80], the regression coefficients and an appropriate model (5.7) are determined for which the coefficient of determination R2 [81] and the residuals are of acceptable values.

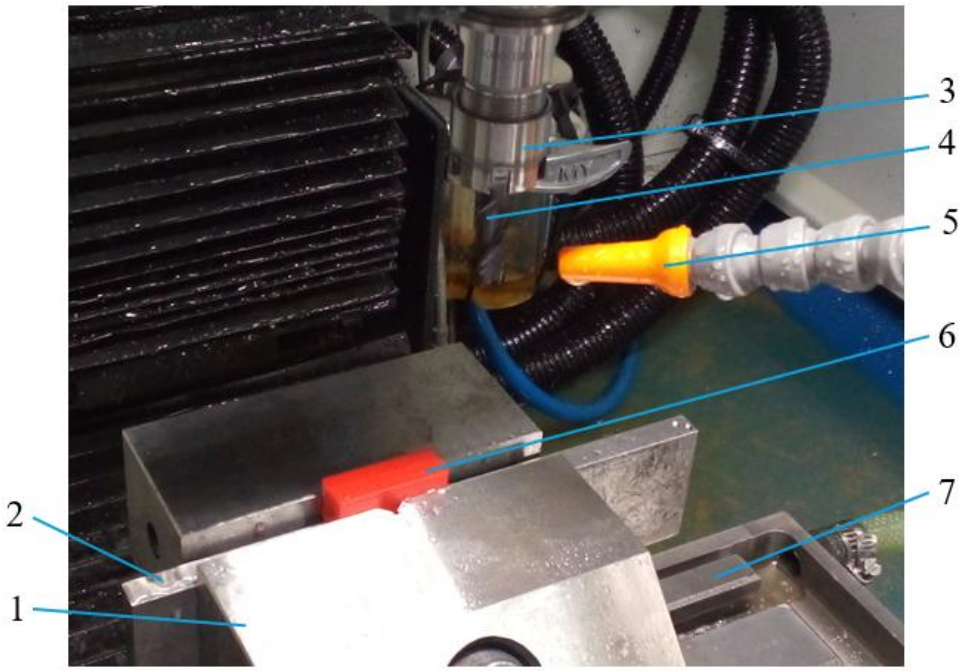
It is emphasized that the level of significance of the regression coefficients also illustrates the level of influence of the corresponding independent variables on the dependent variable, respectively, in the technological conditions considered, the influence of the feed per tooth, the cutting speed or the adjustment feed, as well as other elements – characteristics of the processed material, geometric parameters of the active part of the cutting tool, etc., as the case may be.

It is mentioned that the regression analysis of a function (5.7), respectively, the verification of the adequacy of the model and the significance of the regression coefficients, is carried out in the stage of determining the regression coefficients.

5.2. Experimental data and regression functions of surface roughness obtained within the PLA program - Face milling

5.2.1. Adjustment and programming of the CNC technological system, levels of independent variables, processing and experimental results in the PLA program - Face milling

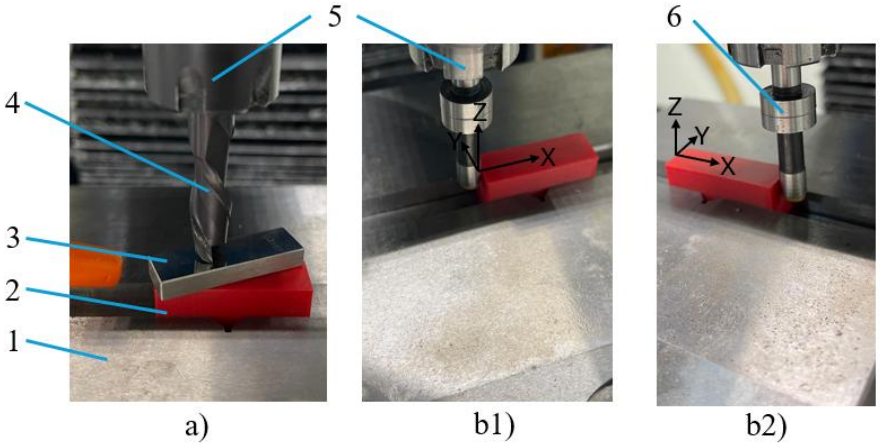
To perform the necessary face milling processing (see Fig. 5.9, PA/ SO – FF), the CNC machining technological system was set up, consisting of specific elements: CNC machining center, orientation - fixing devices, T01 cylindrical face milling cutter, etc. (see also § 5.1.1 e – g, Fig. 5.13).



1 – Precision vice
2 – Orientation plate
3 – Collet chuck
4 – End mill T01
5 – Coolant nozzle
6 – PA part
7 – CNC table

Fig. 5.13. Elements of the CNC milling technological system

Next, dimensional setting of the technological system was carried out in the (X, Y) plane and along the Z-axis (see also § 5.1.1-i), so that the working coordinate system was associated with the workpiece, as shown in Fig. 5.14.



1 – Precision vice
2 – PA part
3 – Orientation plate
4 - End mill T01
5 - Collet chuck
6 – Magnetic probe

Fig. 5.14. Zero setting of the technological system for face milling :
a) along Z axis ; b1) și b2) (X, Y) plane

The levels of independent variables and the content of the experiences were determined in relation to the methodological elements in § 5.1.3 - a, c, as presented in Tables 5.8 and 5.9.

5.2.2. Analysis of experimental results and regression functions regarding the roughness of the surface obtained within the PLA program - Face milling

(1) Analysis of experimental results

Within the PLA – Frontal Milling program carried out (see § 5.2.1), the experiences with no. of order i = 1, 2, …, 23 are grouped so that, in each group, the cutting speed, V_c, is constant, and the feed per tooth, f_z, is increasing variable (see also Annex), namely:

V_c= 56.55 m/min and f_z = 0.0222 - 0.2275 mm/tooth (i = 1, 5, 10, 15, 20),

V_c= 65.29 m/min and f_z= 0.0192 - 0.1970 mm/tooth (i = 2, 6, 11, 16, 21),

V_c= 75.40 m/min and f_z = 0.0298 - 0.0953 mm/tooth (i = 7, 12, 17),

V_c= 87.06 m/min and f_z= 0.0144 - 0.1478 mm/tooth (i = 3, 8, 13, 18, 22),

V_c= 105.5 m/min and f_z= 0.0125 - 0.1280 mm/tooth (i = 4, 9, 14, 19, 23).

For each of the groups of experiences considered, the experimental dependencies Ra(f_z) and Rz(f_z) are considered as shown in Fig. 5.16 - 5.20 (see also Annex).

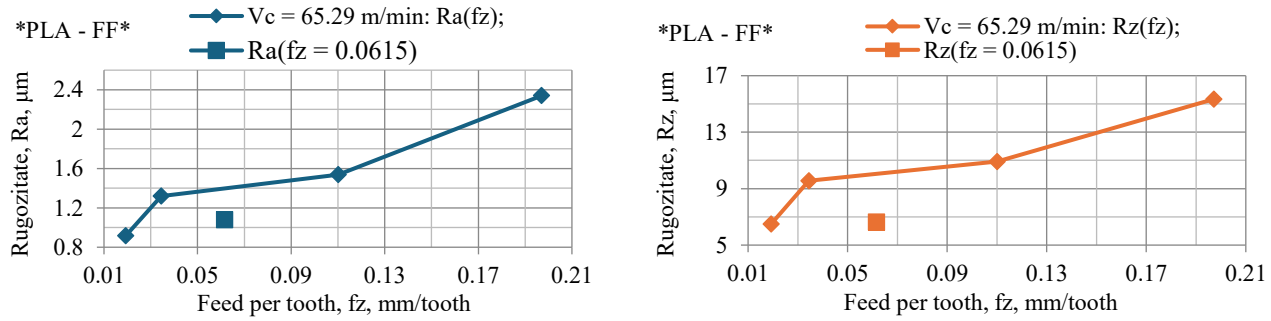


Fig. 5.17. Experimental dependencies: Ra(f_z) and Rz(f_z) for machining with V_c= 65.29 m/min

It is found that, within the above groups of experiences, the roughness parameters Ra and Rz vary similarly to the feed rate f_z, except for some cases [V_c; Y(f_z)]: [56.55; Ra(0.1271)], [65.29; Rz(0.0615)], [87.06; Rz(0.0258) and Rz(0.0825)], [100.5; Ra(0.04), Rz(0.04) and Rz(0.128)].

A comparative analysis of the roughness of printed horizontal surfaces and the roughness of horizontal surfaces processed by front milling, based on the mean effective values of the roughness parameters Ra and Rz, highlights the positive influence of machining by cutting, except for the case [V_c; Y(f_z)]: [75.4; Ra(0.0953) and Rz(0.0953)], where Ra(0.0953) = 4.6603 µm and Rz(0.0953) = 34.326 µm, as shown in Fig. 5.21, 5.22 respectively (see Tables 5.5, 5.9 and Annex).

It is appreciated that, in the case of [V_c; 〚Y(f_z)]: [75.4; Ra(0.0953) and Rz(0.0953)], the Ra and Rz parameters of the surface machined by face milling are of higher values than the values corresponding to the other surfaces machined with V_c= 75.4 m/min and different feeds per tooth, as well as than the values corresponding to the printed surfaces, due to the significant influence of the variation of some characteristics of the machined material.

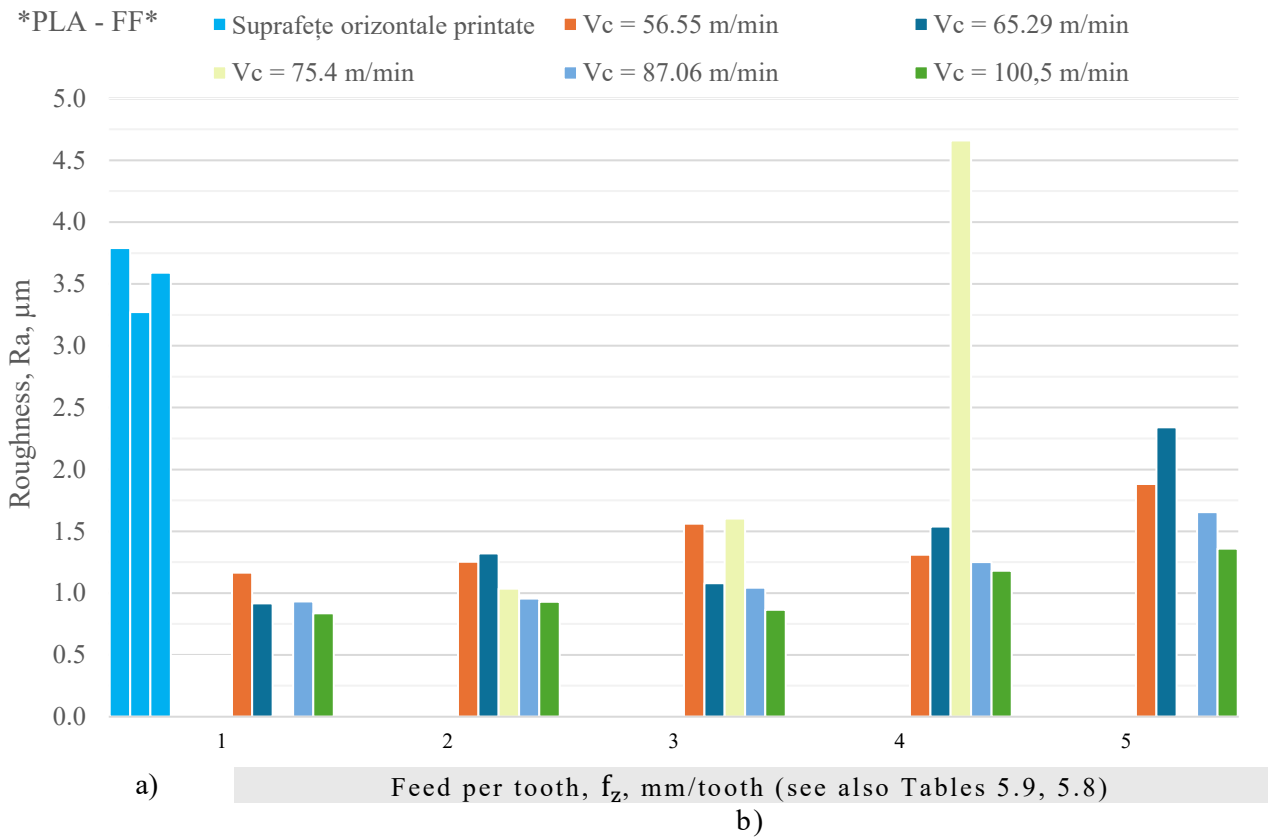


Fig. 5.21. Comparative average values of the roughness Ra of some horizontal surfaces: a) printed (see also Table 5.5), b) processed by front milling (see also Table 5.9, Fig. 5.16 – 5.20)

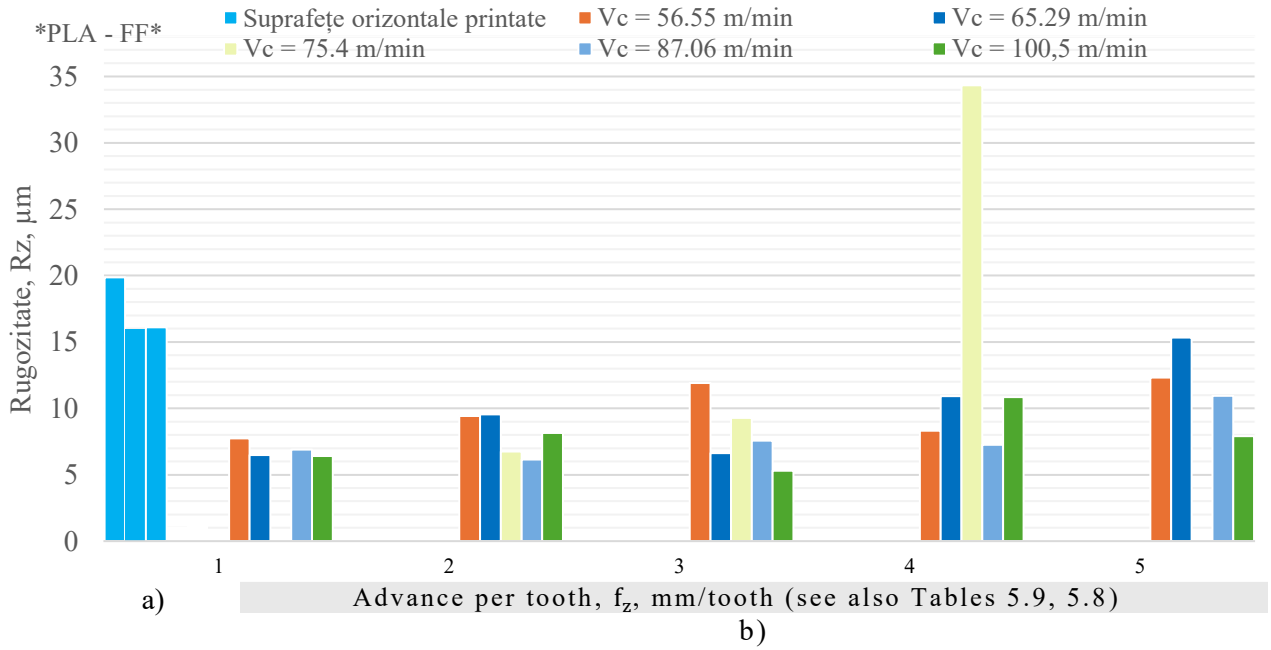


Fig. 5.22. Comparative average values of the roughness Rz of some horizontal surfaces: a) printed (see also Table 5.5), b) processed by front milling (see also Table 5.9, Fig. 5.16 – 5.20)

(2) Machined surface roughness regression functions

In a first stage, monovariable regression functions of machined surface roughness, Ra = Ra(f_z) and Rz = Rz(f_z) of *linear type, power,* etc. were determined [80]. These were analyzed based on the value of the coefficient of determination R^2 [81], as well as in relation to the trend of evolution of the experimental values of the parameters Ra and Rz as a function of the feed per tooth.

The linear and power regression functions Ra = Ra(f_z) and Rz = Rz(f_z) determined are presented in the Annex no. 1.6, and a series of examples in Fig. 5.23 - 5.27.

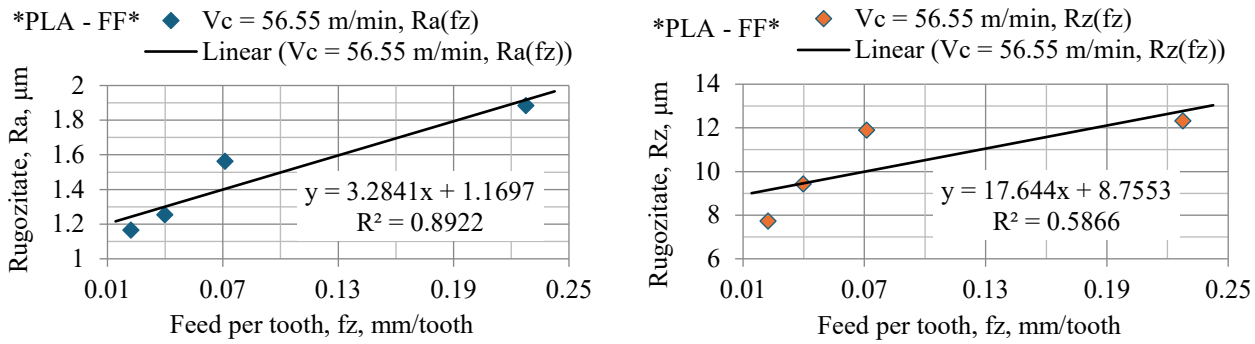


Fig. 5.24. Monovariable regression functions Ra(f_z) și Rz(f_z), *linear* and *power* type, when V_c = 56,55 m/min

It is appreciated that the results of the presented analysis support the choice of the analytical model (5.2).

The calculation of the regression coefficients and the regression analysis regarding the objective machined surface roughness regression functions (5.2) were performed in relation to the methodological elements in § 5.1.3 - e, f. The main data are presented in the Annexes.

A synthesis regarding the regression coefficients b_j and A_j, the machined surface roughness regression functions, Ra (f_z, V_c) and Rz (f_z, V_c), the R* indicators for estimating the adequacy of the regression function model and the R_j indicators for estimating the significance of the b_j regression coefficients are presented below.

PLA Program - Face Milling

Roughness Ra of machined surface		Roughness Rz of machined surface	
b_0 = 0.311947		b_0 = 2.221847	
b_1 = 0.1707	(5.19)	b_1 = 0.144828	(5.24)
b_2 = -0.08377		b_2 = -0.072611	
A_0 = 26.694434		A_0 = 125.141954	
A_1 = 0.293191	(5.20)	A_1 = 0.248753	(5.25)
A_2 = -0.582502		A_2 = -0.504909	
$Ra = 26.6944F^{0.2931}n_c^{-0.5825} <=> Ra = 11.2681f_z^{0.2931}V_c^{-0.2893}$	(5.21)	$Rz = 125.1419F^{0.2487}n_c^{-0.5049} <=> Rz = 57.8758f_z^{0.2487}V_c^{-0.2561}$	(5.26)
R^* = 0.5768	(5.22)	R^* = 0.4193	(5.27)
R_0 = 7.7031		R_0 = 320.2991	
R_1 = 3.4599	(5.23)	R_1 = 2.0413	(5.28)
R_2 = 0.9919		R_2 = 0.6108	

5.3. Experimental data, roughness regression functions and surface dimension obtained within the PLA program - Cylindrical milling

5.3.1. Adjustment and programming of the CNC technological system, levels of independent variables, processing and experimental results in the PLA program - Cylindrical milling

To perform the necessary cylindrical milling operations (see Fig. 5.9, PA/ SV1, 2; C – FC), the technological system was set up and adjusted to dimension, similar to the working method presented in § 5.2.1 (see also 5.1.1-i).

The levels of the independent variables and the content of the experiments were determined in relation to the methodological elements in § 5.1.3 - a, c, as presented in Tables 6.10 and 5.11.

Through the editing interface of the CNC Machining Center, the CNC Cylindrical Milling Program was activated, as presented in Fig. 5.29. It is mentioned that the address instructions S and F, S... and, respectively, F... , are programmed in the preparation stage of each experiment i. Thus, for example, before the execution of the experiment i = 2, at which the values of the speed and feed rate are 2248 rpm and, respectively, 171 mm/min (see Tables 5.10, 5.11), S2248 and F171 are programmed, by direct editing.

Under the above conditions, for each experiment/printed part i, i = 1, 2, ..., 30, the vertical objective surfaces SV1, SV2 were processed by cylindrical milling, successively, and the objective dimension C was also achieved, implicitly (see Fig. 5.9, PA/ SV1, 2; C – FC; Fig. 5.30).



Fig. 5.30. A machined part, PA/ SV1, 2; C – FC

Next, for each processed part i, i = 1, 2, ..., 30: the roughness of the SV1 surface and the distance C between the SV1, SV2 surfaces were measured, respectively, the mean effective values of the roughness parameters Ra and Rz of the SV1 surface were determined, as well as the mean effective values of the dimension C (see also § 5.1.1-g, h, j, k and 5.1.3-d).

Thus, the determined effective values of the roughness parameters Ra and Rz, as well as of the dimension C within the PLA - Cylindrical Milling program are as shown in Table 5.11.

5.3.2. Analyses of experimental results, roughness and dimension regression functions regarding surfaces machined within the PLA program - Cylindrical milling

(1) Analysis of experimental results

Within the PLA - Cylindrical Milling program performed (see § 5.3.1), similar to the analysis presented in § 5.2.2-(1), the experiments with sequence numbers i = 1, 2, …, 25 were structured into five groups, so that, in each group: the cutting speed, V_c, is constant, namely, of value 56.5, 65.26, 75.4, 87.06 or 100.5 – in m/min; the feed per tooth, f_z, is variable, successively, namely of values 0.02, 0.0331, 0.0547, 0.0906 and 0.15 - in mm/tooth.

A comparative analysis of the roughness of printed vertical surfaces and the roughness of vertical surfaces processed by cylindrical milling, through the mean effective values of the roughness parameters Ra and Rz, highlights the positive influence of machining, as shown in Fig. 5.34 and 5.35.

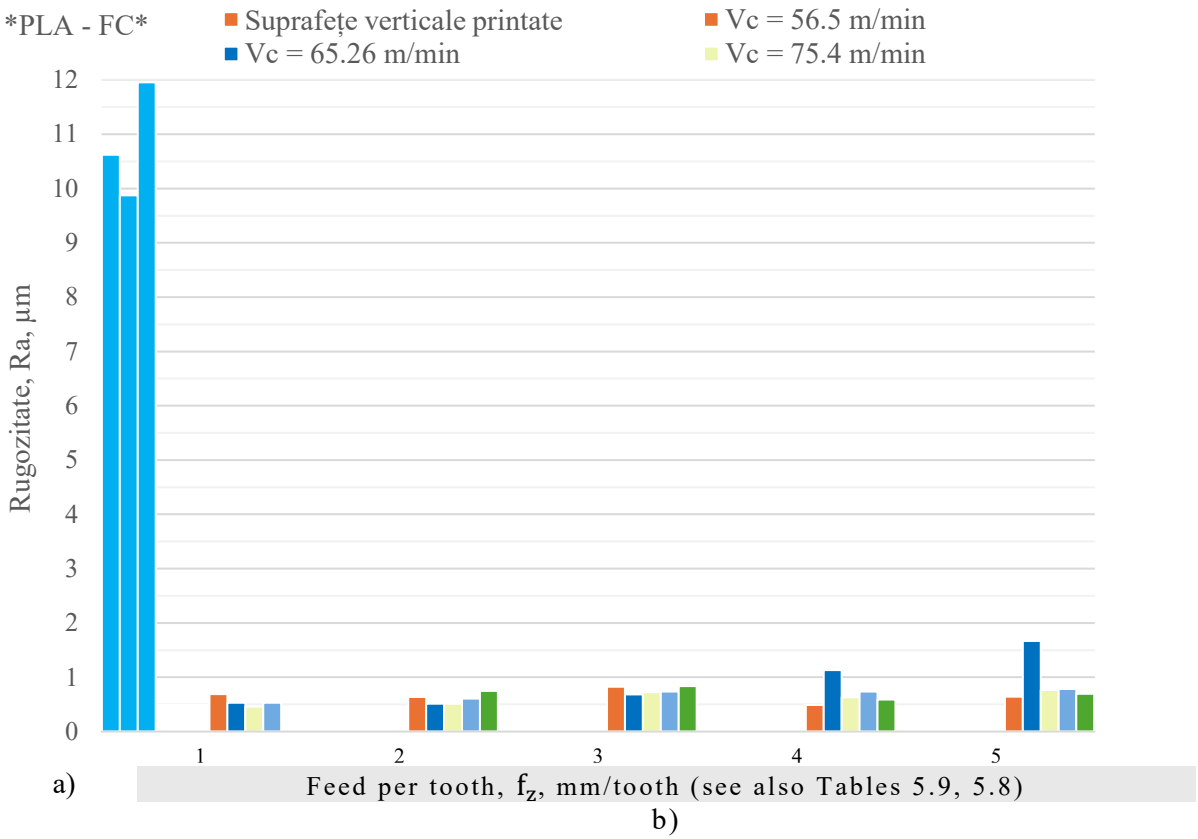


Fig. 5.34. Comparative values of the roughness Ra of some vertical surfaces: a) printed (see also Table 5.5), b) processed by cylindrical milling (see also Table 5.11)

(2.1) Multivariable roughness regression functions

The calculation of the regression coefficients and the regression analysis on the objective machined surface roughness regression functions (5.2) were performed in relation to the methodological elements in § 5.1.3 - e, f. The main data are presented in the Annex.

A summary of the regression coefficients b_j and A_j, the machined surface roughness regression functions (SV1), Ra (f_z, V_c) and Rz (f_z, V_c), the R* indicators for estimating the adequacy of the regression function model and the R_j indicators for estimating the significance of the b_j regression coefficients is presented below.

PLA program - Cylindrical milling

Roughness Ra of machined surface		Roughness Rz of machined surface	
b_0 = -0.42228065 b_1 = 0.115964972 b_2 = 0.014942892	(5.29)	b_0 = 1.3920374 b_1 = 0.06516512 b_2 = 0.005063467	(5.34)
A_0 = 0.817120701 A_1 = 0.230180111 A_2 = 0.103697822	(5.30)	A_0 = 5.03206958 A_1 = 0.12934694 A_2 = 0.035138477	(5.35)
$Ra = 0.8171 f_z^{0.2301} V_c^{0.1036}$	(5.31)	$Rz = 5.032 f_z^{0.1293} V_c^{0.0351}$	(5.36)
R^* = 0.5437	(5.32)	R^* = 0.8905	(5.37)
R_0 = 17.6468 R_1 = 2.6616 R_2 = 0.0441	(5.33)	R_0 = 332.0268 R_1 = 1.4552 R_2 = 0.0087	(5.38)

(3) Comparative analysis of some experimental values of the roughness of surfaces processed within the PLA program - Cylindrical milling

Within the PLA - Cylindrical Milling program, for experiments i = 1, 2, 3, the roughness parameters Ra and Rz of the machined plane surface SV2 were also determined (see Fig. 5.9, PA/ SV1, 2; C - FC). The values of the parameters Ra and Rz of the two machined parallel plane surfaces SV1 and SV2 are presented in Table 5.12.

The percentage error [83, 84, 85], ΔY%, of the experimental value, Y, in relation to the calculated value, Y_calc, respectively, is considered as an indicator of comparative analysis,

$$\Delta Y\ \% = 100\ (Y - Y_{calc})/Y_{calc} \text{ in } \%,\ Y = Ra, Rz \qquad (5.44)$$

where, Ra_{calc} și $Rz_{calc}$are determined by using the corresponding regression function (5.31) and, respectively, (5.36), and the considered quantities are determined for each i = 1, 2, 3.

The calculation of the errors ΔRa % and ΔRz %, by applying rel. (5.44) to the analyzed experimental data Ra, Rz (Table 5.12) and the corresponding values Ra_{calc}, respectively, Rz_{calc}– determined by using the function (5.31), respectively, (5.36), is presented in the Annexes 1.7 and 1.8, as well as, synthetically, in Table 5.13.

Based on the comparative analysis of the data associated with the flat surfaces SV1 and, respectively, the flat surfaces SV2, the following is found:

• in the experiments/experimental pieces i = 1, 2, the absolute values of the percentage errors Δ Ra % and Δ Rz %, associated correspondingly with the flat surfaces SV1 and, respectively, with the flat surfaces SV2, differ by up to two orders of magnitude;

• in the experiment/experimental piece i = 3, the absolute values of the percentage errors Δ Ra % and Δ Rz %, associated correspondingly with the flat surfaces SV1 and, respectively, with the flat surfaces SV2, are of the same order of magnitude;

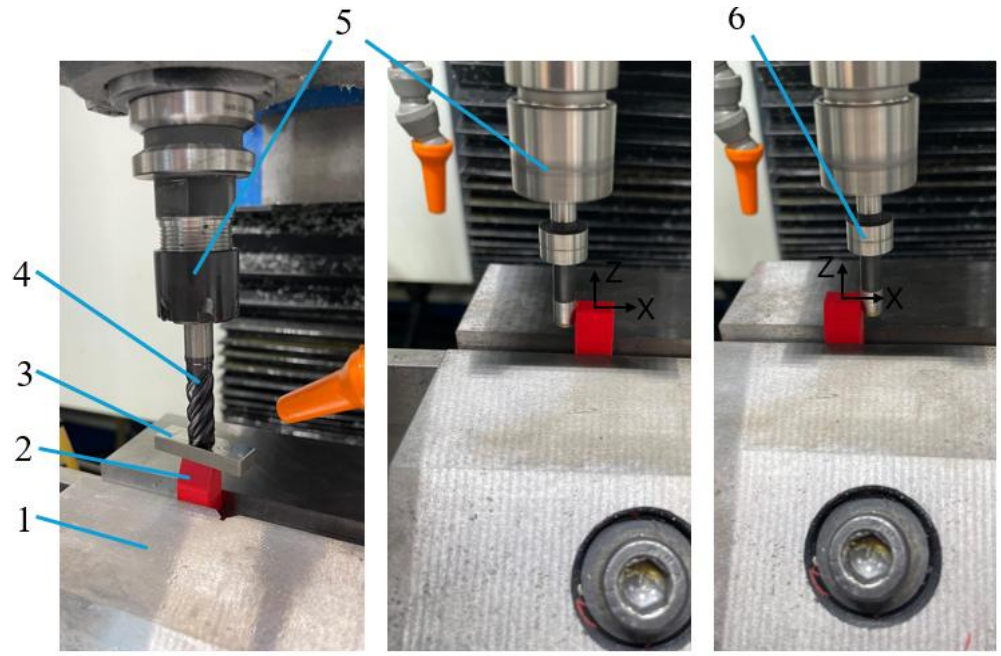
• at the level of the group of experiments/experimental pieces, i = 1, 2 and 3, the absolute values of the percentage errors Δ Ra % and, respectively, Δ Rz % associated correspondingly with the flat surfaces SV1 and, respectively, with the flat surfaces SV2, are variable in different value ranges.

It is considered that a possible cause of the differences between the compared roughness values is, in most cases, the structural variation of the material of the experimental pieces.

5.4. Experimental data, surface roughness regression functions obtained within the PLA program - Cylindrical-face milling

5.4.1. Adjustment and programming of the CNC technological system, levels of independent variables, processing and experimental results in the PLA program - Cylindrical-face milling

To perform the necessary face milling processing (see Fig. 5.9, PB/ SI – FCF), the CNC milling technological system was set up, similar to the working method presented in § 5.2.1, with the mention that the face milling cutter is T02 – with a tip radius of 0.5 mm (see also § 5.1.1 e – g).
The technological system was adjusted, in the (X, Y) plane and in the Z direction (see also § 5.2.1, 5.1.1-i,), so that the working coordinate system is associated with the workpiece, with the origin at the intersection point between the symmetry axis of the four vertical surfaces and the upper horizontal surface, as shown in Fig. 5.39.



1 – Precision vise

2 – PB part

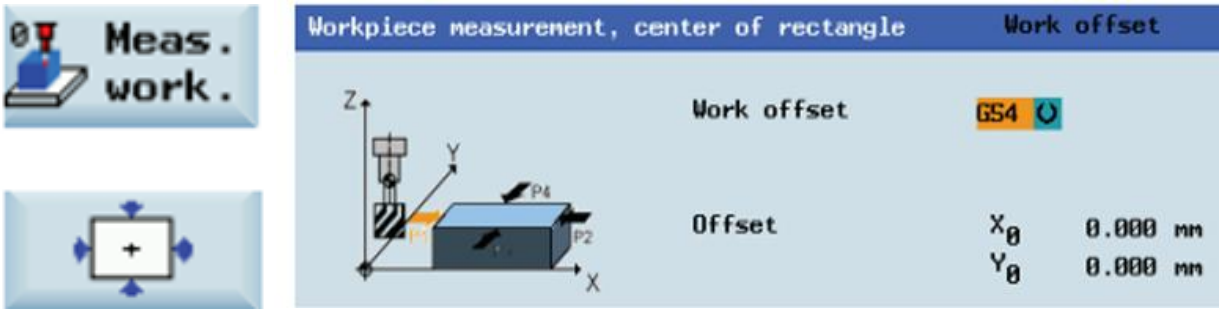
3 – Shim plate

4 – End mill T02

5 – Collet chuck

6 – Magnetic probe

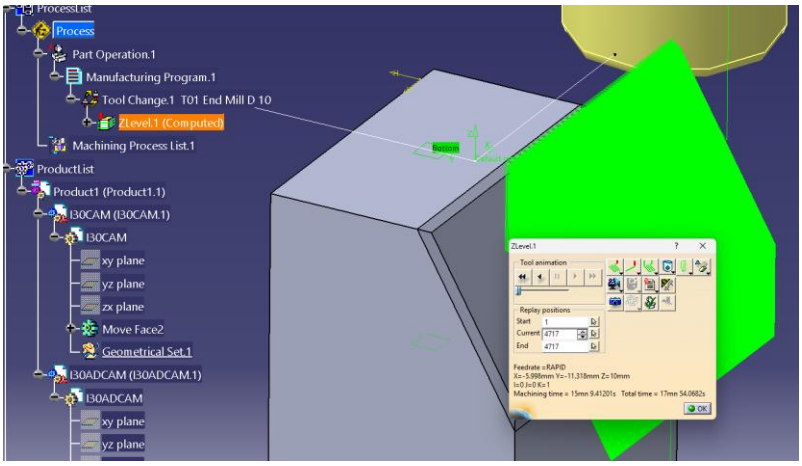
a) b1) b2)



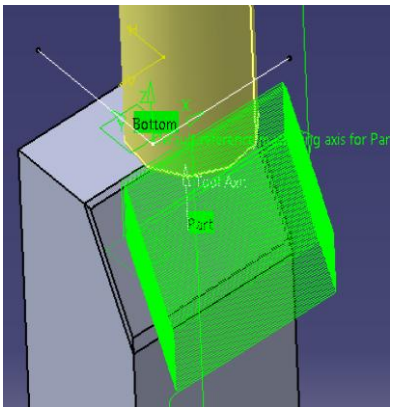
c)

Fig. 5.39. Zero setting of the technological system for cylindrical-face milling:
a) along Z axis; b1) și b2) (X, Y) plane ; c) origin setup elements

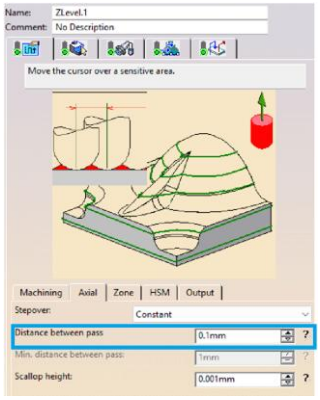
The CNC program for cylindrical-face milling was generated within the Catia V5R21 application (Fig. 5.44-2).



a)



b)



c)

Fig. 5.44-2. Generating the CNC Program for Cylindrical Face Milling in the Catia V5R21 application: a) elements regarding the programming interface, b) Simulation of the machining path, c) ZLevel Command

The constant levels of the feed per tooth, f_z, and the cutting speed, V_c, respectively, the corresponding values of the speed, n_c, and the feed speed, F, the levels of the independent variable - the axial adjustment feed, p, as well as the content of the experiments were determined in relation to the methodological elements of § 5.1.3 - a, c, as presented in Tables 5.14 and 5.15. It is noted that the values of the feed per tooth, f_z, and the cutting speed, V_c,, were chosen from the levels from cylindrical milling that led to relatively low values of the roughness of the machined surface and the basic time.

Under the above conditions, for each experiment/printed part i, i = 1, 2, ..., 5, depending on the corresponding level of the independent variable - the axial feed rate p (see Table 5.14), the CNC Program Cylindrical-face milling was activated, through the CNC Machining Center interface, and the objective inclined plane surface was machined by cylindrical-face milling (see also Fig. 5.9, PB/ SI – FCF; Fig. 5.41).
Next, at each machined surface i, i = 1, 2, ..., 5, the roughness was measured, respectively, the effective values of the roughness parameters Ra and Rz were determined (see also § 5.1.1-j, 5.1.3-d).

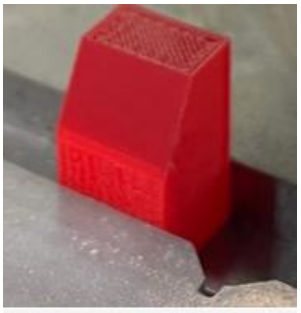
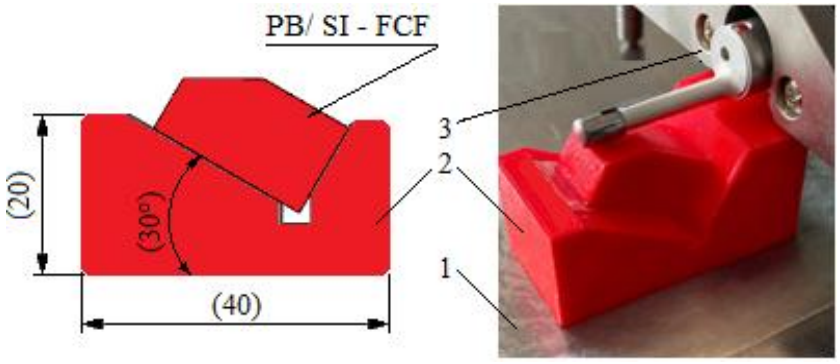


Fig. 5.41. A machined part, PB/ SI; FCF

The following is mentioned: the orientation prism (Fig. 5.46) was designed and produced by 3D printing from PLA and finishing milling; double-sided adhesive tape was used to fix the orientation prism to the control board and the measuring part to the orientation prism – interposed between the elements in question.



1 – Control plate

2 – Orientation prism

3 – Digital surface roughness tester

Fig. 5.42. Elements of the inclined surface roughness measurement system of PB/ SI - FCF parts

5.4.2. Analysis of experimental results and regression functions regarding the roughness of the machined surface within the PLA program - Cylindrical-face milling

(1) Analysis of experimental results

Within the PLA program - Cylindrical-face milling performed (see § 5.4.1), similar to those presented in § 5.2.2 - (1) and 5.3.2 - (1), the experimental dependencies Ra(p) and Rz(p) were determined

(see Annex 1.10).

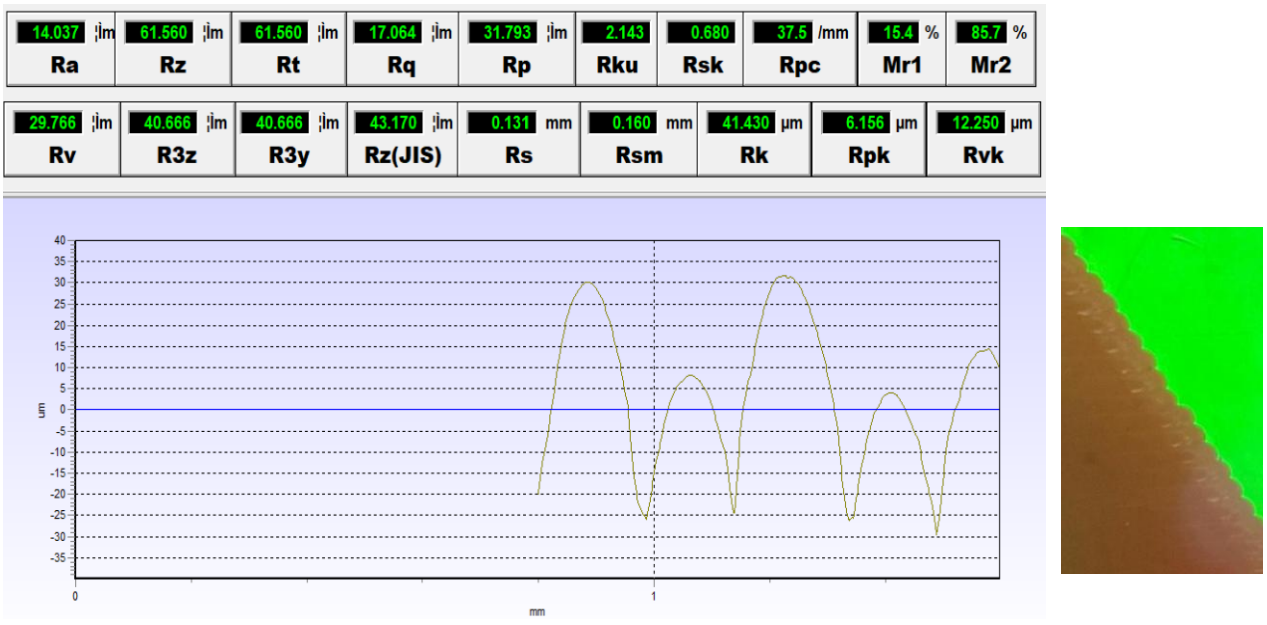
It is found that the roughness parameters Ra and Rz vary similarly to the axial feed p, except for the cases (p; Ra): (0.01; 1.297), (p; Rz): (0.01; 10.399) and (p; Rz): (0.1; 7.8626) (see also Tables

5.15 – 5.19).

Thus, it is appreciated that the factors influencing the roughness of inclined flat surfaces processed in the PLA program - Cylindrical-face milling, which can be highlighted, in relation to the above, are: the variation of the axial feed p, because, in most cases, the roughness parameters Ra and Rz vary monotonically increasing with the axial feed p; the variation of some characteristics of the processed material - in cases where the correlation between Ra, Rz and p is not found, because other elements - geometric parameters of the cutting tool, characteristics of the coolant-lubricant, etc. - are considered to have insignificant variation.

A comparative analysis of the roughness of printed inclined surfaces and the roughness of inclined surfaces processed by cylindrical-face milling, based on the effective mean values of the roughness parameters Ra and Rz, highlights the positive influence of machining by cutting, as also shown in

Fig. 5.47 - 5.50 (see Tables 5.5, 5.15 and Annex).



a) b)

Fig. 5.43. Elements regarding the roughness of a printed inclined surface: a) roughness profile and values of roughness parameters/ Ra = 14.037 µm, Rz = 61.65 µm etc. (see also Table 5.5); b) microscopic view (see also Fig. 5.6)

Chapter 6. Research on the roughness and dimensional precision of 3D printed and CNC milled PETG parts

In order to determine the actual characteristics of roughness and dimensional accuracy in PETG parts to be analyzed in comparison with the roughness and dimensional accuracy achieved in PLA parts, research was conducted on the roughness and dimensional accuracy of 3D printed PETG parts processed by CNC milling under conditions similar to those in which the research on milling processing of PLA parts was carried out (presented in chapter 5).

Thus, below, some mentions will be presented regarding the reference elements in chapter 5 and, mainly, the specific results of the research conducted on the roughness and dimensional accuracy of 3D printed PETG parts processed by CNC milling.

6.1. Characteristics of research processes and systems for determining roughness and dimensional precision of 3D printed PETG parts obtained by CNC milling

6.1.1. Research programs, PETG material, types of parts, elements of experimental research processes and technological systems

(1) Research programs

The PETG - Face Milling, PETG - Cylindrical Milling and PETG - Cylindrical-Face Milling research programs have been developed through which, under defined conditions:

• a series of parts are 3D printed from PETG;

• in the printed parts, flat surfaces of different positions are processed by CNC milling, namely, *horizontal* flat surfaces - by face milling and *vertical* flat surfaces - by cylindrical milling, respectively, *inclined* flat surfaces - by cylindrical-face milling, as the case may be;

• the roughness parameters Ra and Rz are modeled and analyzed, as well as the dimensional accuracy related to some flat surfaces of the printed parts and, accordingly, related to the *horizontal, vertical, inclined flat* surfaces processed by CNC milling.

6.1.2. Evaluation of roughness and dimensional precision of 3D printed parts made of PETG material

For a series of 3D printed parts made of PETG material, the effective roughness parameters, Ra*, Rz*, of horizontal (frontal), vertical (lateral) and inclined surfaces were determined, as well as the effective distance, C*, between two vertical (plane, parallel) surfaces [see also § 6.1.1 – (4)]. The results are presented in the Annex. The effective roughness parameters Ra* and Rz*, as well as the effective average values of the C* dimension are also presented in Tables 6.2 and 6.3.

The following are noted (see Tables 6.2, 6.3 and Annex):

• for *horizontal* surfaces, the roughness parameter Ra* has effective values in the roughness classes

N 9 - 10 (Ra 6.3 - 12.5), and for *vertical and inclined* surfaces, the parameter Ra* has effective values in the roughness classes N10 - 11 (Ra 12.5 - 25) [94];

• the dimension C* has effective values in the tolerance class IT12 [95].

6.1.3. Roughness and dimension modeling elements associated with surfaces processed by face, cylindrical and cylindrical-face milling in 3D printed parts made of PETG material

The elements of modeling the roughness and dimension associated with the surfaces processed by milling in 3D printed parts from PETG, respectively,

a) the process variables, dependent and independent, including elements regarding the parameters of the cutting regimes,

b) the analytical models for the regression functions of roughness and dimension of the processed surfaces,

c) the levels of the independent variables and the specific structural elements of the experiments,

d) the effective values of the dependent variable,

e) the calculation of the regression coefficients,

f) the regression analysis

are as presented in § 5.1.3.

6.2. Experimental data, roughness and surface size regression functions obtained in the PETG - Face Milling and PETG - Cylindrical Milling research programs

6.2.1. Adjustment and programming of the CNC technological system, levels of independent variables, processing and experimental results in the PETG - Face Milling and PETG - Cylindrical Milling research programs

To perform the necessary face milling and cylindrical milling operations

(see Fig. 6.1, PA/ SO – FF, SV1, 2; C - FC), the CNC machining technological system was set up and adjusted to dimension, similar to the working method presented in § 5.2.1 (see also 5.1.1-i).

Under the above conditions, for each experiment/printed part i, i = 1, 2, ..., 30, the objective *horizontal* plane surfaces SO and vertical SV1, SV2, SO - by front milling, SV1 and SV2 - in relation to the objective dimension C - by cylindrical milling were processed successively (see Fig. 6.1, PA/ SO – FF, SV1, 2; C – FC; Fig. 6.3). Next, for each processed part i, i = 1, 2, ..., 30: the roughness of the SV1 surface and the distance C between the SV1, SV2 surfaces were measured, respectively, the mean effective values of the roughness parameters Ra and Rz of the SV1 surface were determined, as well as the mean effective values of the dimension C [see also § 6.1.1 - (4), 6.1.3 - d)].

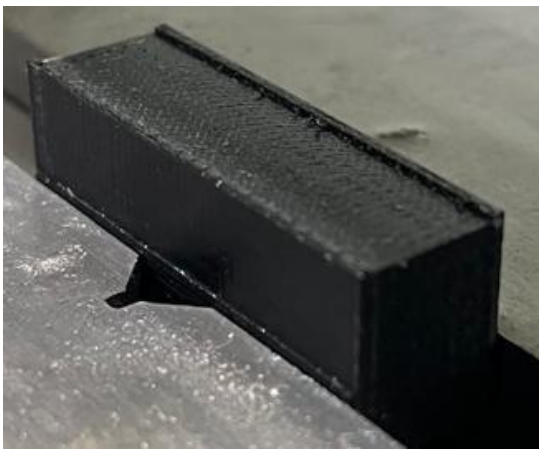


Fig. 6.3. A machined part,
PA/ SO - FF, SV1, 2; C - FC

Thus, the effective values of the roughness parameters Ra and Rz, as well as the C dimension within the PETG - Face Milling and PETG - Cylindrical Milling programs are as shown in Table 6.5.

6.2.2. Analysis of experimental results and regression functions regarding the roughness of the obtained surface within the PETG program - Face milling

(2) Multivariable machined surface roughness regression functions

The main data regarding the calculation of regression coefficients and regression analysis (see also § 6.1.3,5.1.3 – e, f) regarding the objective machined surface roughness regression functions, the PETG program - Frontal milling, are presented in the Annexes 2.2 and 2.3.

A summary regarding the regression coefficients b_j and A_j, the machined surface roughness regression functions, Ra (f_z, V_c) and Rz (f_z, V_c), the R* indicators for estimating the adequacy of the regression function model and the R_j indicators for estimating the significance of the b_j regression coefficients is presented below.

PETG Program - Front Milling

Roughness Ra of machined surface		Roughness Rz of machined surface	
$b_0 = 0.893405305$		$b_0 = 2.7610969$	
$b_1 = 0.129072259$	(6.1)	$b_1 = 0.105808318$	(6.6)
$b_2 = -0.028418347$		$b_2 = -0.009821479$	
$A_0 = 12.06063883$		$A_0 = 39.08306138$	
$A_1 = 0.256196904$	(6.2)	$A_1 = 0.210020061$	(6.7)
$A_2 = -0.197212207$		$A_2 = -0.068157221$	
$Ra = 12.0606 f_z^{0.2561} V_c^{-0.1972}$	(6.3)	$Rz = 39.083 f_z^{0.21} V_c^{-0.0681}$	(6.8)
$R^* = 0.19$	(6.4)	$R^* = 0.1736$	(6.9)
$R_0 = 53.0818$		$R_0 = 488.4161$	
$R_1 = 2.2158$	(6.5)	$R_1 = 1.4344$	(6.10)
$R_2 = 0.1074$		$R_2 = 0.0123$	

Since R* < 1 [see rel. (6.4) and (6.9)] and $R_j > 1$, j = 0, 1, R_2 < 1 [see rel. 6.5) and (6.10)], it follows that the regression function model (6.3) and (6.8) is adequate (R* < 1) and that, under the technological conditions considered, the feed per tooth, as well as other elements – characteristics of the processed material, geometric parameters of the active part of the cutting tool, etc. – are factors with a significant influence on the roughness of the processed surface ($R_2 > 1$, $R_0 > 1$), and the cutting speed is a factor with a lower influence on the roughness of the processed surface ($R_2 < 1$).

6.2.3. Analyses of experimental results, roughness regression functions and dimension regression functions regarding surfaces obtained within the PETG program - Cylindrical milling

(2.1) Multivariable roughness regression functions

The main data regarding the calculation of regression coefficients and regression analysis (see also § 6.1.3, 5.1.3 – e, f) regarding the regression functions of the objective machined surface roughness, the PETG program - Cylindrical Milling, are presented in the Annexes 2.4 and 2.5.

A summary of the regression coefficients b_j and A_j, the machined surface roughness regression functions (SV1), Ra (f_z, V_c) and Rz (f_z, V_c), the R* indicators for estimating the adequacy of the regression function model and the R_j indicators for estimating the significance of the regression coefficients b_j are presented below.

PETG Program - Cylindrical Milling

Roughness Ra of machined surface		Roughness Rz of machined surface	
b_0 = -0.473496515		b_0 = 1.214950039	
b_1 = 0.09062813	(6.11)	b_1 = 0.035405115	(6.16)
b_2 = 0.023658248		b_2 = 6.98378E-05	
A_0 = 0.516501079		A_0 = 4.124588437	
A_1 = 0.17988874	(6.12)	A_1 = 0.07027599	(6.17)
A_2 = 0.164178981		A_2 = 0.000484647	
$Ra = 0.5165 f_z^{0.1798} V_c^{0.1641}$	(6.13)	$Ra = 4.1245 f_z^{0.0702} V_c^{0.0004}$	(6.18)
R^* = 3.6490	(6.14)	R^* = 14.721	(6.19)
R_0 = 20.4374		R_0 = 204.8358	
R_1 = 1.4974	(6.15)	R_1 = 0.3478	(6.20)
R_2 = 0.102		R_2 = 1.35363E-06	

It is found that $R^* > 1$ [see rel. (6.14) and (6.19)], $R_0 > 1$, $R_1 > 1$ or $R_1 < 1$, $R_2 < 1$ [see rel. (6.15) and (6.20], respectively, under the technological conditions considered: the feed per tooth is a factor with a significant influence on the roughness parameter Ra, but with a lower influence on the roughness parameter Rz; the cutting speed is a factor with a lower influence on the roughness of the machined surface ($R_2 < 1$); other elements – characteristics of the machined material, geometric parameters of the active part of the cutting tool, etc. – have a significant influence on the roughness of the machined surface ($R_0 > 1$), so that, among these, other independent variables can be selected to extend the analytical model of the regression function.

6.3. Experimental data, surface roughness regression functions obtained within the PETG program - Cylindrical-face milling

6.3.1. Adjustment and programming of the CNC technological system, levels of independent variables, processing and experimental results in the PETG program - Cylindrical-face milling

To perform the necessary face milling processing (see Fig. 6.1, PB/ SI – FCF), the CNC milling technological system was set up and adjusted to dimension, similar to the working method presented in § 6.2.1, with the mention that the face milling cutter is T02 – with a tip radius of 0.5 mm (see also § 5.2.1, 5.1.1 e – i).

The CNC program Cylindrical-face milling was generated within the Catia V5R21 application (Fig. 5.45, Annex).

The constant levels of the feed per tooth, f_z, and the cutting speed, V_c, respectively, the corresponding values of the speed, n_c, and the feed rate, F, the levels of the independent variable - the axial adjustment feed, p, and the content of the experiments were determined based on the elements in § 6.1.3 - a, c (§ 5.1.3 - a, c), as well as in § 5.4.1, as presented in Table 6.8.

Under the above conditions, for each experiment/printed part i, i = 1, 2, ..., 5, depending on the corresponding level of the independent variable - the axial feed rate p (see Table 6.8), the CNC Program Cylindrical-frontal Milling was activated, through the CNC Machining Center interface, and the objective *inclined* plane surface was machined by cylindrical-frontal milling (see also Fig. 6.1, PB/ SI - FCF; Fig. 6.4).
Next, for each machined surface i, i = 1, 2, ..., 5, the roughness was measured, respectively, the effective values of the roughness parameters Ra and Rz were determined, similar as presented in § 5.4.1.
Thus, the effective values of the roughness parameters Ra and Rz within the PETG program - Cylindrical-frontal Milling are as presented in Table 6.8.

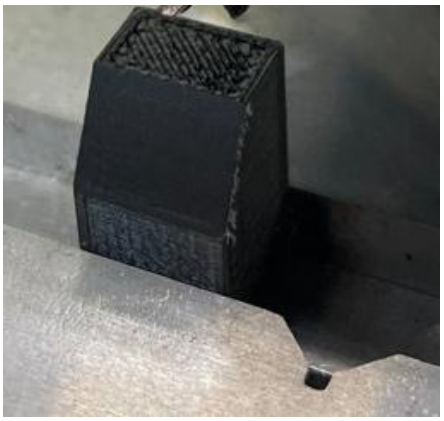


Fig. 6.4. A machined part, PB/ SI – FCF

Table 6.8. PETG Program - Cylindrical Face Milling: Levels of Independent and Control Variables, Content of Experiences and Actual Values of Ra and Rz Roughness Parameters

Nr. exp., i	f_z, mm/tooth; V_c, m/min (n_c, rot/min; F, mm/min)	p, mm	Inclined flat surface							
			Actual values of roughness parameters determined based on roughness measurement, µm						Effective values average, µm	
			Ra 1	Rz 1	Ra 2	Rz 2	Ra 3	Rz 3	Ra	Rz
1	0.0331; 87.0551 (3463; 573)	0.01	0.879	6.082	0.928	8.014	0.851	6.082	0.886	6.726
2		0.0177	0.937	5.366	0.977	6.44	1.045	7.346	0.9863	6.384
3		0.0316	1.495	9.063	1.114	5.533	1.518	6.726	1.3756	7.1073
4		0.0562	1.098	7.298	0.95	6.654	0.984	6.13	1.0106	6.694
5		0.10	1.188	6.583	1.437	7.942	1.238	6.535	1.2876	7.02

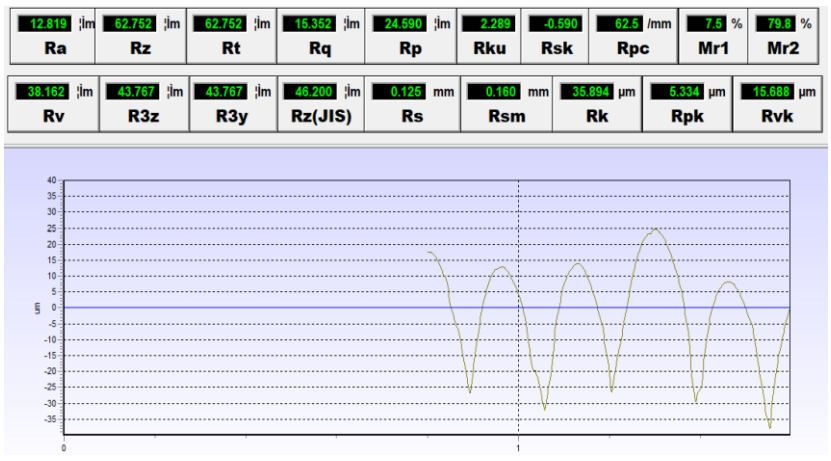
6.3.2. Analysis of experimental results and regression functions regarding the roughness of the obtained surface within the PETG program - Cylindrical-face milling

(1) Analysis of experimental results

Within the PETG - Cylindrical-face milling program performed (see § 6.3.1), similar to those presented in § 5.2.2 - (1) and 5.3.2 - (1), the experimental dependencies Ra(p) and Rz(p) were determined (see Annex no. 2.7). It is found that the roughness parameters Ra and Rz vary similarly to the axial feed p, except for the cases (p; Ra): (0.0316; 1.3756), (p; Rz): (0.01; 6.726) and (p; Rz): (0.0316; 7.1073) (see also Tables 6.8 - 6.12).

It is appreciated that, in most cases, the roughness parameters Ra and Rz vary monotonically increasing with the axial feed p, and in cases where this relationship is not observed, the main cause is the variation of some characteristics of the processed PETG material.

A comparative analysis of the roughness of printed inclined surfaces and the roughness of inclined surfaces processed by cylindrical-face milling, based on the mean effective values of the roughness parameters Ra and Rz, highlights the positive influence of machining, as shown in Fig. 6.4 – 6.11 (see also Tables 6.2, 6.8, Annex).

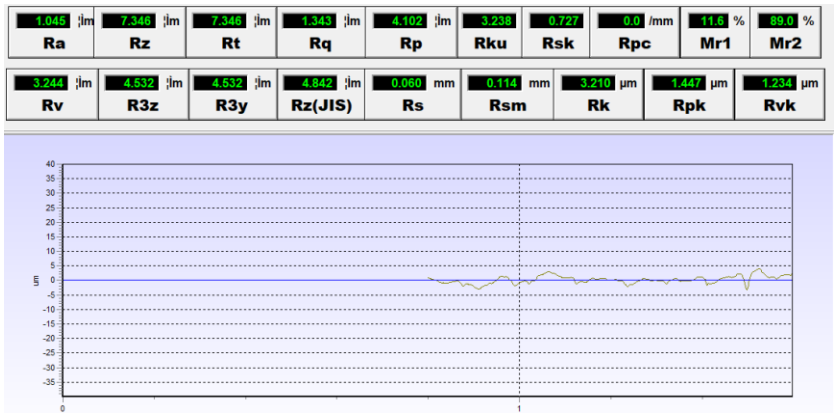


a)

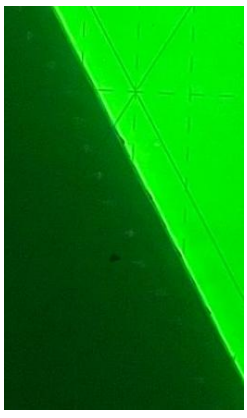


b)

Fig. 6.4. Elements regarding the roughness of a printed inclined surface: a) roughness profile and values of roughness parameters/ Ra = 12.819 µm, Rz = 62.752 µm etc. (see also Table 6.2); b) microscopic view (see also Fig. 5.6)



a)



b)

Fig. 6.5. Elements regarding the roughness of an inclined surface machined by end milling: a) roughness profile and values of roughness parameters/ Ra = 1.045 µm, Rz = 7.345 µm etc. (see also Table 6.8); b) microscopic view (see also Fig. 5.6)

(2) Machined surface roughness regression functions

In relation to the trend of the evolution of the experimental values of the parameters Ra and Rz of the surfaces processed by cylindrical-face milling as a function of the axial feed rate of regulation (see § 6.3.2 – (1)), the surface roughness functions (inclined plane) Ra and Rz are analyzed and determined as regression functions (5.7) for which the coefficient of determination $\mathbf{R^2}$and the residuals are of acceptable values [see also § 6.1.3 -b), 5.1.3 - (b2)].

For this purpose, variants of the regression functions Ra (p) and Rz (p) are determined, of the form (5.7), based on pairs of values/coordinates (p, Ra)i and, respectively, (p, Rz)i from the experimental ones and, in each case, the value of the coefficient of determination R^2 and the values of the relative error ΔY% (rel. 5.45) are analyzed. From the variants of the regression functions Ra (p) and, respectively, Rz (p) thus determined, the variant Ra (p) and, respectively, the variant Rz (p) are selected for which the coefficient of determination $\mathbf{R^2}$ and the corresponding associated relative errors are of acceptable values.

The considered analysis highlights the fact that, in the group of five experiments/experimental pieces, $i = \overline{1,5}$ (see Tables 6.9, 6.11), as well as in other groups of experiments (see Annex), some values of the roughness parameters Ra and Rz, respectively, the values of the coefficient of determination $\mathbf{R^2}$ and of some relative errors are inappropriate. It is considered that a possible cause is represented, in most cases, by the structural variation of the material of the experimental pieces.

Thus, in relation to the above, it is considered that the regression functions of the roughness of the machined surface (inclined plane) Ra and Rz are appropriate (see Tables 6.10 and 6.12):

$$\mathrm{Ra} = 1.6417\mathrm{p}^{0.1341} \tag{6.26}$$

$$\mathrm{Rz} = 7.8776\mathrm{p}^{0.053} \tag{6.27}$$

Chapter 7. Research on the development of technological models in PLA for the manufacture of silicone molds applied to the casting of polyurethane resin products

Silicone molds are developed to produce rubber gaskets, medical implants made of PMMA (polymethylmethacrylate), decorative objects made of resin, sweets, etc. (see also § 1.2, 101]).

Research on the development of technological models from PLA for the manufacture of silicone molds applied to the casting of parts made of polyurethane resin was carried out as follows.

7.1. Defining elements and stages - framework of research

Two technological models MT1 and MT2 are defined that participate in the manufacturing, by casting, of silicone molds, MS1 and MS2, respectively; molds MS1 and MS2 are used for manufacturing from polyurethane resin, by casting, of products P1 and P2, respectively.

The relationships resulting from the above determinations can be expressed in the form:

$$MT1 \Rightarrow MS1,\ MS1 \Rightarrow P1;\ MT2 \Rightarrow MS2,\ MS2 \Rightarrow P2 \qquad (7.1)$$

The present research mainly aims at the development of technological models in PLA, MT1 and MT2, the evaluation of the influence of the roughness and dimensional accuracy of the MT1 and MT2 models in the manufacture of silicone molds MS1 and MS2, respectively, based on the analysis of the characteristics of the products P1 and P2, made of polyurethane resin, by casting, in the silicone molds considered. (Fig. 7.1).

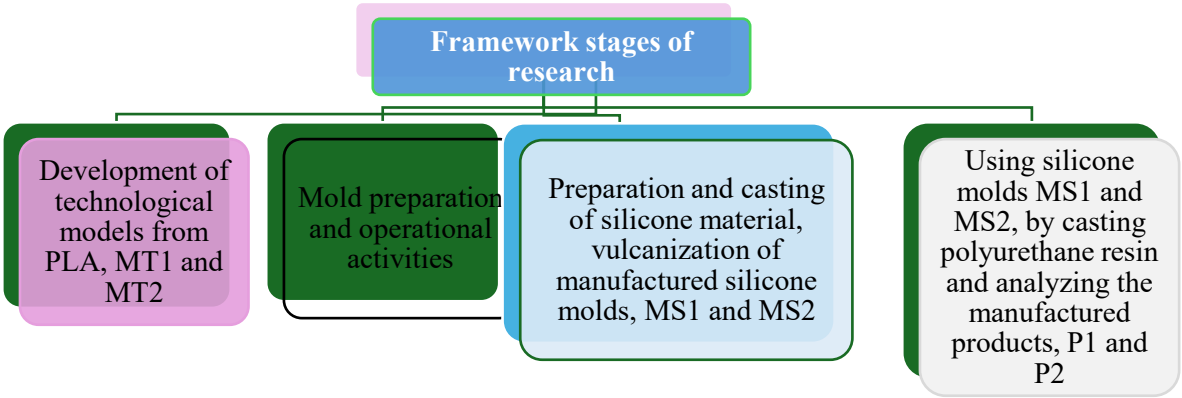


Fig. 7.1. Framework stages of research

7.2. Development of technological models from PLA

(a) Designing technological models

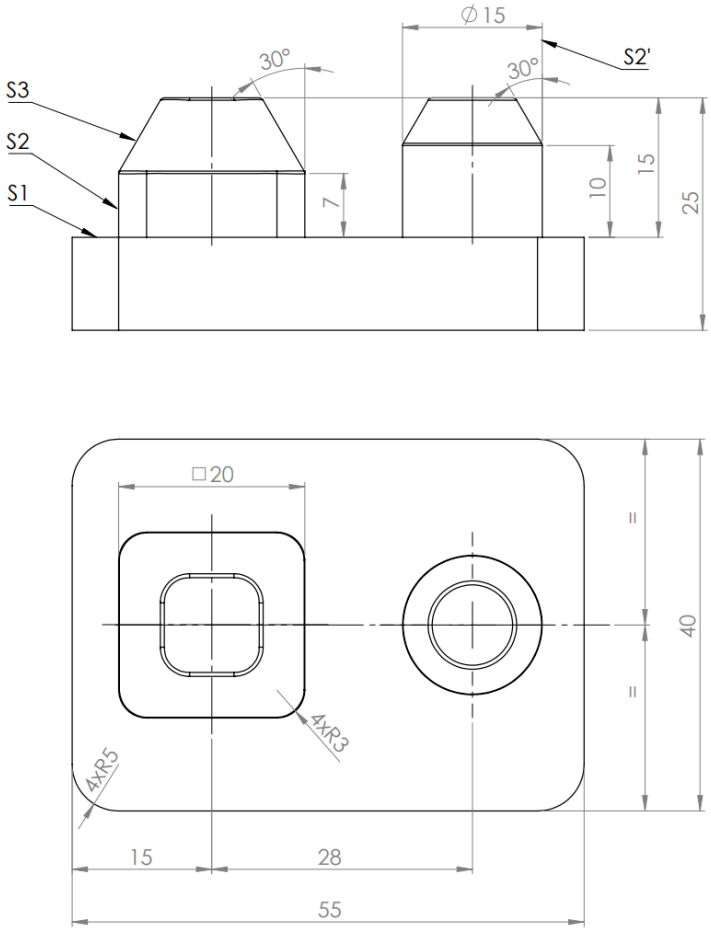
The technological models MT1 and MT2 were designed using the SolidWorks application, so that:

• the constituent material is PLA - presented in § 5.1.1 - b, with the particularity that it is red for MT1, respectively, green for MT2;

• the component surfaces are of nominal shapes, dimensions and positions - presented in Fig. 7.2;

• the technological model MT1 is manufactured by 3D printing;

• the technological model MT2 is manufactured by 3D printing and CNC milling of the main surfaces.



MT1: 3D printing manufacturing; MT2: manufacturing by 3D printing and CNC milling of S1, S2, S2′, S3 surfaces – corresponding tu a total machining allowance of 0,5 mm

Fig. 7.2. Prescribed geometric characteristics of technological models MT1 and MT2

(c) CNC milling of the main surfaces of the MT2 technological model

The CNC machining center, the cylindrical end mills, the coolant – lubrication, the orientation and fixing devices, as well as the establishment of the technological system for CNC milling processing are as presented in § 5.1.1 d – g and 5.2.1.

The CNC Milling program was generated within the Catia V5R21 application (Fig. 7.3 – 7.5), with the following mentions:

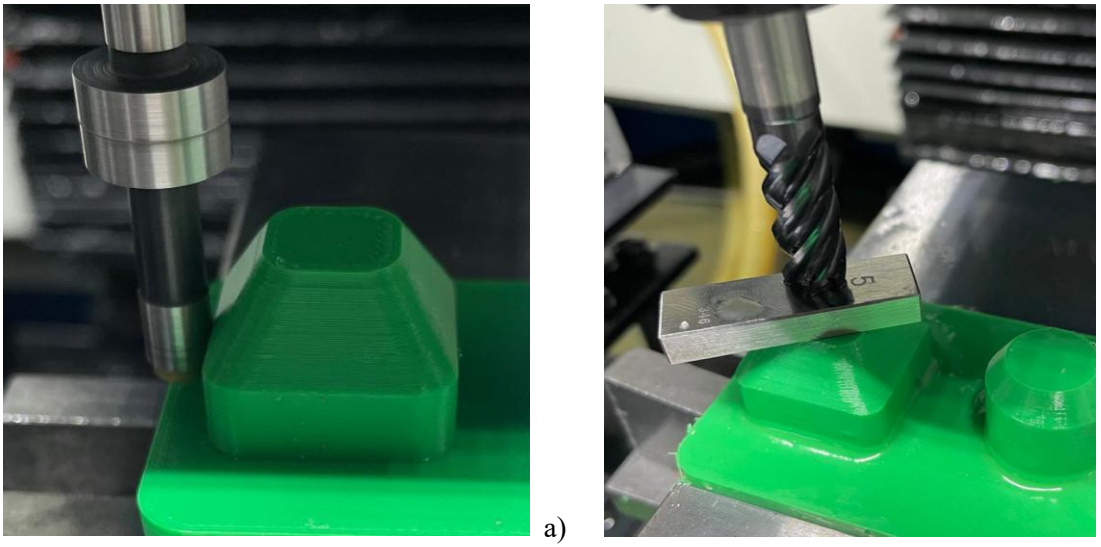
• two origins of the coordinate systems were used, symmetrical with respect to the four flat surfaces S2 (Fig. 7.3);

• corresponding to each elementary surface, the total machining allowance, with the value of 0.5 mm, was distributed: 0.3 mm - to the roughing phase/one pass, respectively, 0.2 mm - to the finishing phase/one pass;

• in the phases of *Part Operation.3*, the T01 cylindrical-face milling cutter was used, and in the phases of *Part Operation.2* - the T02 cylindrical-face milling cutter, with entry-exit in a circular arc (circular interpolation).

The technological system was adjusted to dimension (see also § 5.1.1 - i, 5.2.1, 5.4.1/ Fig. 5.44), so that the working coordinate system OXYZ is associated with the workpiece, with the origin O at the intersection point between the axis of symmetry of the four vertical flat surfaces S2 and the horizontal flat surface S4, practically: adjustment in the horizontal plane (X, Y) - by using a

magnetic probe and centering in four points (Fig 7.5 - a); adjustment in the Z direction - by using a contact path between the front surface of the tool and the horizontal surface S4 printed (first origin), respectively, processed by milling (second origin) (Fig 7.5 - b).

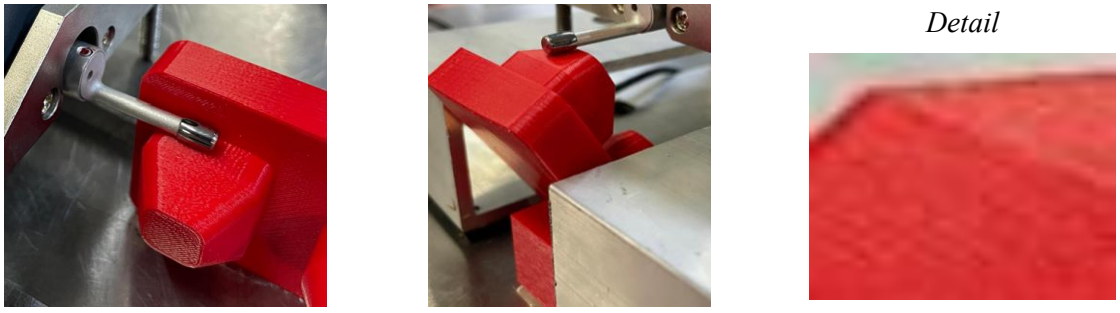


a) b)

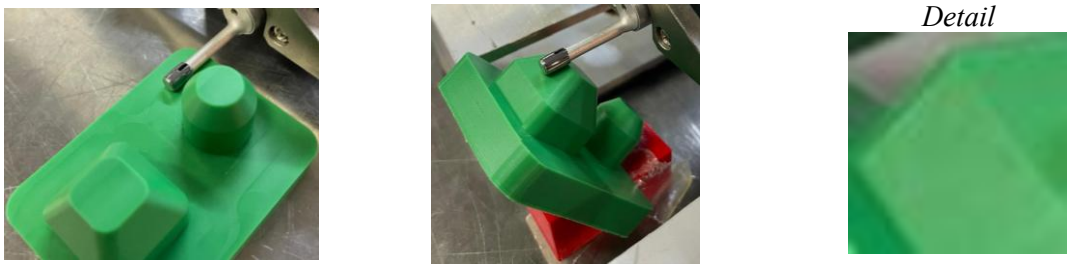
Fig. 7.5. Zero adjustment of the technological system: a) in the (X, Y) plane, b) in the Z direction

(d) Effective geometric characteristics of the manufactured technological models MT1 and MT2

The technological model MT1, manufactured from PLA by 3D printing, and the technological model MT2, manufactured from PLA by 3D printing and CNC milling of the main surfaces (see above), were subjected to roughness measurement operations and main dimensions (see also § 5.1.1 - g, j, k, 5.1.3 - d; Fig. 5.4.6; Fig. 7.6).



Technological model MT1



Technological model MT2

Fig. 7.6 Roughness measurement on: technological models MT1 (after printing), MT2 (after milling)

The determined effective values of the roughness parameters Ra and Rz, as well as the measured dimensions, are as presented in Tables 7.1 and 7.2.
The following are highlighted (see Tables 7.1, 7.2):

• for the MT1 technological model, the roughness parameter Ra has effective values at surfaces S1, S2 and S3, in roughness classes N9 (Ra 6.3), N10 (Ra 12.5) and, respectively, N11 (Ra 25) [94], and the dimensions
l and d have effective values in tolerance classes IT 15 and, respectively, IT 16 [95];
• in the MT2 technological model, the roughness parameter Ra has effective values at surfaces S1 and S2, S3, in roughness classes N7 (Ra 1.6), respectively, N8 (Ra 3.2) [94], and the dimensions l and d have effective values in tolerance classes IT 7 and, respectively, IT 8 [95].
It is found that all the evaluated geometric characteristics Ra, Rz, l and d of the MT2 technological model are of higher precision than the precision of the corresponding characteristics of the MT1 technological model.

7.3. Manufacturing of silicone molds

a. Main components and characteristics of silicone material

The silicone material used for the manufacture of MS1 and MS2 silicone molds is a two-component mixture of RTV ZA-22 Addition Silicone and a ZA-22 Catalyst (curing agent), with the main characteristics indicated by the manufacturer [88], as shown in Table 7.3.

Table 7.3. Characteristics of silicone material [88]

(1) Silicone type (color), (2) Hardening agent, (3) Mixing ratio of components, (4) Mixture viscosity (5) Density, (6) Mixing time of components; Working/pouring time (at 23°); Curing - demoulding time (at 23°)					(7) Shore A hardness (after 24 hours), (8) Dimensional variation (after 24 hours), (9) Detail reproduction, (10) Elongation at break, (11) Tensile strength, (12) Tear strength)					
(1); (2)	(3)	(4)	(5)	(6)	(7)	(8)	(9)	(10)	(11)	(12)
RTV ZA-22 Addition Silicone (Blue);	RTV ZA-22 Addition Silicone (Blue);	cP	g/cm^3	min	Sh A	%	µm	%	N/mm^2	N/mm
		4000 ± 300	1,15	2; 14 - 17; 90 - 120	21 ± 2	- 0,05	2	380 ± 20	4 ± 0.2	20 ± 1

b. Preparation of molds, preparation and casting of silicone material, vulcanization and demolding of manufactured molds MS1 and MS2

The casting molds are prepared by positioning and fixing with double-sided adhesive tape the technological models MT1 and MT2, each in a graduated beaker (Fig. 7.7 - a); the necessary silicone material is produced by mixing 200 ml of silicone and 200 ml of catalyst (Fig. 7.7 - b), in a graduated beaker; the silicone material is poured into the molds (Fig. 7.7 - c).


a)

b)

c)

Fig. 7.7. Elements regarding the manufacture of silicone molds: a) one of the molds, b) silicone and catalyst, c) pouring the silicone material into molds and vulcanizing the produced molds

The curing (hardening) time of the molds was approx. 2.5 hours, at ambient temperature. Finally, the molds were (manually) demolded from the casting molds (Fig. 7.8).

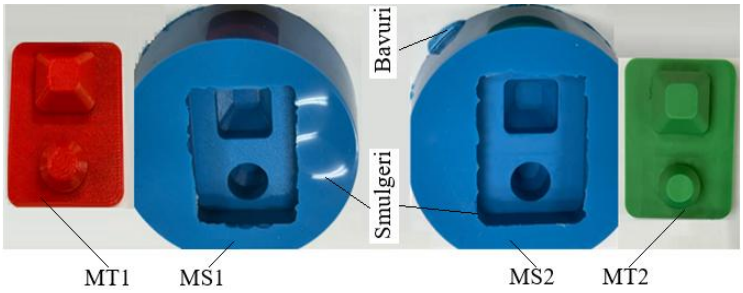


Fig. 7:8. Manufactured molds and models, after demolding: MS1, MT1; MS2, MT2

The following are mentioned:
• in areas of uneven contact between the silicone material and the elements of the casting mold - glass wall and model -, burrs were formed within each mold, and the manual removal of some burrs led to material tearing (see Fig. 7.8);
• to ensure the completion of the curing/vulcanization process, respectively, the stabilization of the characteristics, the manufactured silicone molds, MS1 and MS2, were used after 12 hours after demolding.

7.4. Manufacturing of polyurethane resin parts using silicone molds produced and analysis of experimental results

a) Main components and characteristics of polyurethane resin

In general, polyurethane resin is a polymeric material consisting of several components.

For the present research, a two-component Multicast 1 polyurethane resin was selected and used, with the main characteristics indicated by the manufacturer [89], as shown in Table 7.4.

Table 7.4. Polyurethane Resin Characteristics Multicast 1 [89]

(1) Resin type (color), (2) Hardening agent, (3) Mixing ratio component weights, (4) Mixture viscosity, (5) Working/pouring time; Curing- demoulding time (6) Shore D hardness				
(1); (2)	(3)	(4)	(5)	(6)
Multicast 1 (white-yellowish); ISO Catalyst 2	1:1	mPa.s	min	Sh D
		55 - [35/75]	3 - 6; 75	75

b) Preparation and casting of polyurethane resin, curing and demolding of manufactured parts P1, P2

Mix the Multicast 1 resin with the ISO 2 curing agent in equal parts by mass, which is an exothermic chemical process; pour the polyurethane resin made into the MS1 and MS2 silicone molds (Fig. 7.9-1).



Fig. 7.9-1. Casting parts from polyurethane resin P1 and P2

The castings, P1 and P2, respectively, reached ambient temperature 10 - 15 min before the completion of the curing process; the curing time was 80 min. Finally, the castings P1 and P2 were demolded, manually, from the molds (Fig. 7.9).

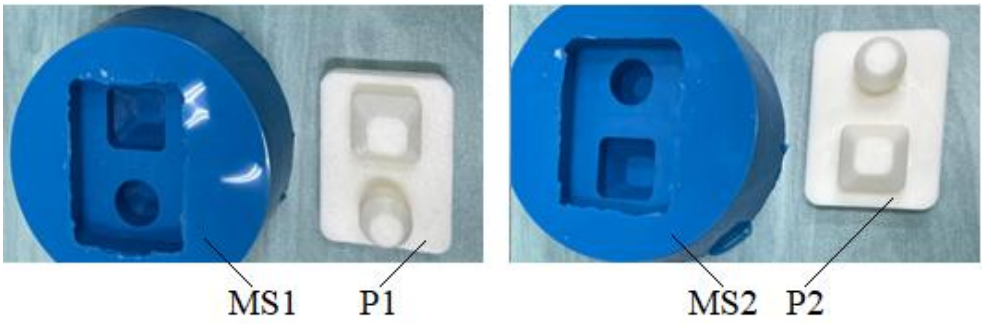


Fig. 7.9-2. Silicone molds and produced parts, after demolding: MS1, P1; MS2, P2

c) Effective geometric characteristics of manufactured parts P1 and P2

The manufactured parts, P1 and P2, were subjected to operations to measure the roughness of the surfaces S1, S2, S3 and the dimensions l and d (see also § 5.1.1 - g, j, k, 5.1.3 - d; Fig. 5.4.6; Fig. 7.10).

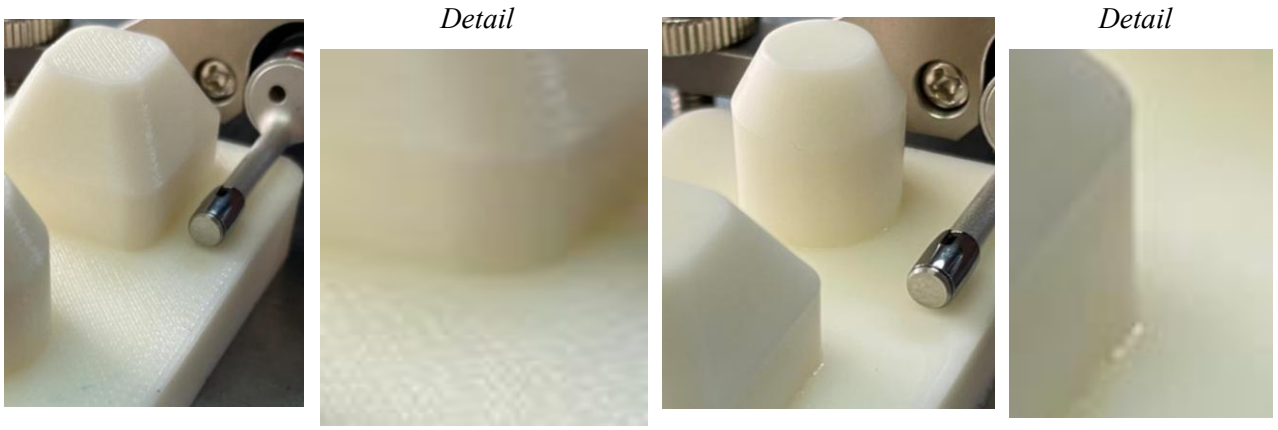


Fig. 7.10. Measurement of the roughness of the main surfaces of manufactured parts P1 and P2

The determined effective values of the roughness parameters Ra and Rz, as well as the dimensions l and d, are as presented in Tables 7.5 and 7.6.

Chapter 8. Research on finite element analysis, fabrication and testing of precision cold bending molds made of PLA and PETG

Research on finite element analysis, fabrication and testing of cold bending molds made of PLA and PETG, which also includes published elements of the author [90], is as follows.

8.1. Defining elements and stages - framework of research

Precision/calibration cold V-bending diagram and die

The cold bending scheme is considered in a precision/calibration V, so that the corresponding defining geometric characteristics of the punch, the active plate and the objective piece, Pg, are equal, namely the apex angles, 90°, the inner connection radii, R, and the outer connection radii, R + g, and the thickness and width of the semi-finished product are equal to the thickness, g, and, respectively, the width, B, of the piece Pg, as shown in Fig. 8.1 (see also Fig.8.2).

The precision/calibration cold bending die, MIV, consists of the active elements, respectively, the punch and the active plate.

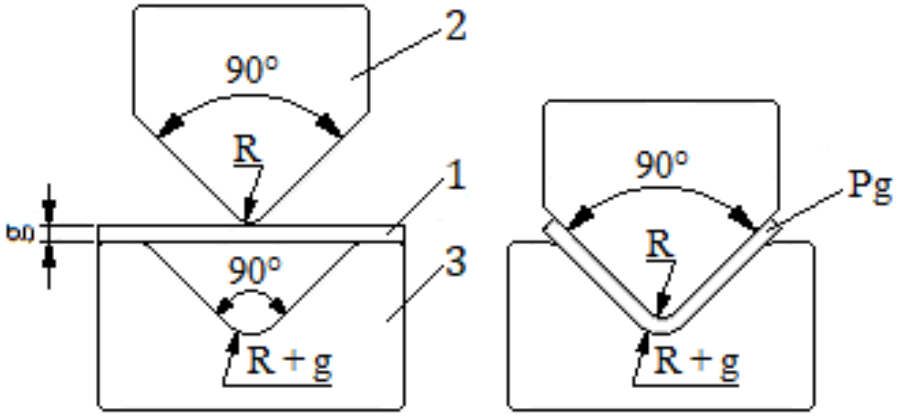


Fig. 8.1. Precision/Calibration Cold V Bending Scheme:
1/ Pg - Semi-finished/Objective Part, 2 – Punch, 3 – Active Plate

Process variables and the structural analysis model

The following are considered as independent process variables:

• thickness, g, of the blank/part Pg, g: 0.5, 1, 2, 3 mm;

• width, B, of the blank/part Pg, B: 15, 20 mm;

• inner radius, R, of the part Pg, R: 2.5 mm, for g: 0.5, 1 mm; R: 3 mm, for g: 2 mm; R: 4 mm, for g: 3 mm;

• material of the punch and the active plate, the same for both elements, PLA and PETG, respectively;

• working stroke, h, of the punch, h: 12.75, 12.55, 11.93, 11.1 mm, corresponding to g: 0.5, 1, 2, respectively, 3 mm;

The dependent process variable(s) are considered, as appropriate: the bending force/plastic deformation, F, in N, or the stress σ, in MPa, or the specific deformation, ε, in %, etc.

8.2. Determining the effective tensile properties of PLA, PETG and Al materials

The effective tensile properties of PLA, PETG and Al materials were determined under the conditions regulated by ISO 527, as follows.

The Epruv-PLA and Epruv-PETG specimens, with the dimensions in Fig. 8.4, were manufactured by 3D printing. The 3D printer, the printing parameters and the other working conditions were as presented in § 5.1.1 - d and, respectively, § 6.1.1 - (4). The Epruv-Al specimens, with the dimensions of 250 x 15 x 2 mm, were produced by cutting and deburring from flat strip.

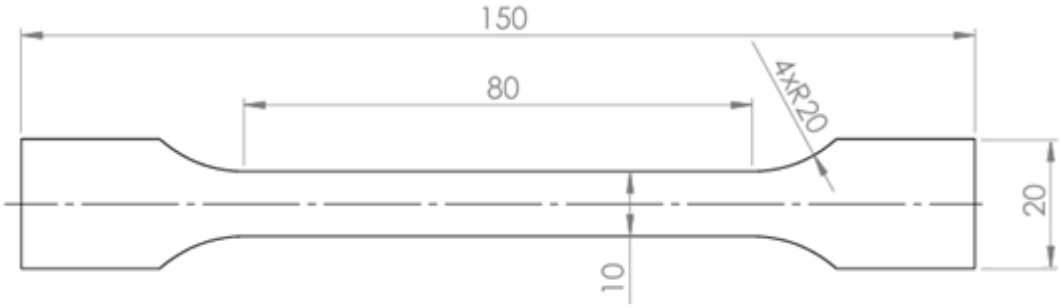
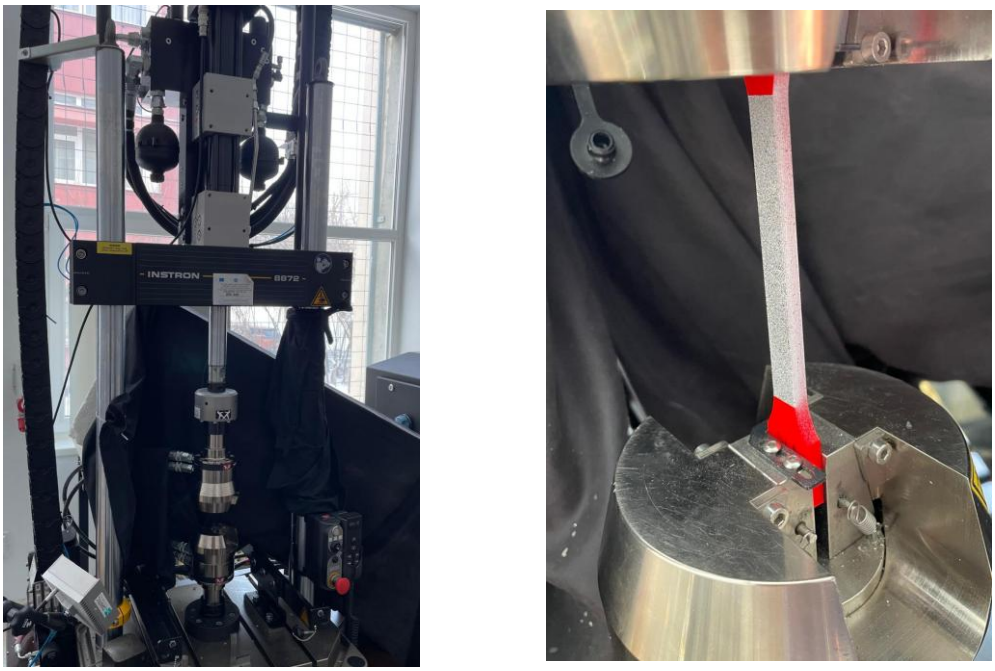


Fig. 8.4. Dimensions of the PLA-Sample and PETG-Sample [8ISO 527]

All specimens were prepared by applying a layer of white paint with black dots on the active surfaces (see Fig. 8.5-b), in order to record the deformation field by the digital image correlation (DIC) method.

The tests were performed on an INSTRON 8872 electrohydraulic universal testing machine (Fig. 8.5), equipped with a Dantec Dynamics Q400 (EduDIC System) device for recording specific deformations by the digital image correlation (DIC) method.



a) b)

Fig. 8.5. Elements regarding tensile testing of PLA, PETG and Al specimens on the INSTRON 8872 electrohydraulic universal testing machine: a) view of the working area, b) details regarding the orientation and fixation of the specimen

8.3. Finite element analysis

Finite Element Analysis, FEA, for prediction and interpretation of data, based on calculations with the Finite Element Method, FEM, regarding the stress-deformation process during precision cold V-bending processing with PLA or PETG molds of some Al parts, was carried out as follows.

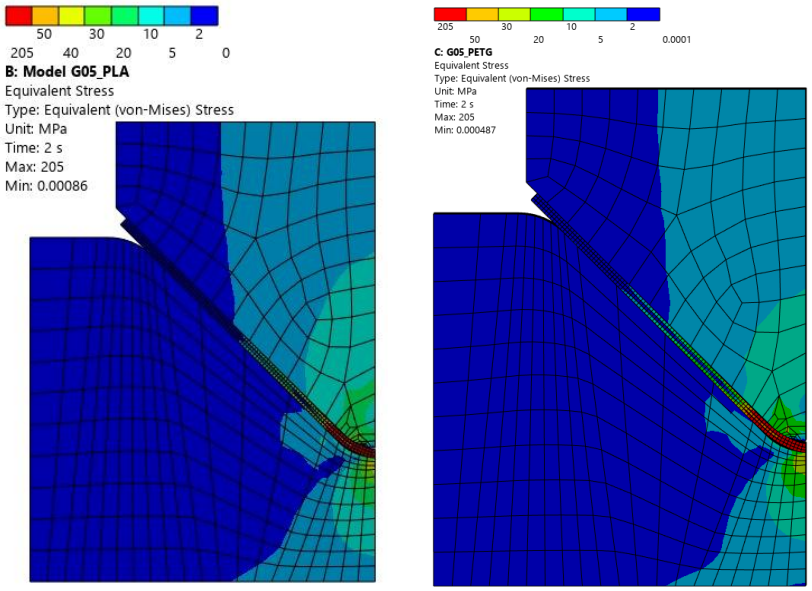
In order to simulate the precision cold V-bending process, for the two materials – PLA and PETG – of the MIV mold and four variants of the part thickness Pg - Pg0.5, Pg1, Pg2, Pg3 (see rel, 8.1) - eight static simulations were designed.

The geometry simplifications, material models, contacts between the interacting elements, discretization, boundary conditions and simulation running parameters are presented.

The simulation of the eight geometry/material cases generated, for each, a map of the distribution of stresses and strains specific to the elements involved, which evolve in time, during the bending process.

A representative von Mises equivalent stress map, in the cases of PLA or PETG active elements and the Pg0.5 part at the end of the stroke, is shown in Fig. 8.17, with the mention that in the areas with low stresses a logarithmic scale representation of the values was chosen.
The following are noted:
• the highest stresses are at the part level, respectively, of 205 MPa - in the case of both PLA and PETG active elements;

• the stresses in the active elements of the mold (PLA or PETG) are significantly lower than those in the part (Al);



Active elements in PLA Active elements in PETG

Fig. 8.17. A map of the von Mises equivalent stresses, in the cases of active elements made of PLA, PETG and Pg0.5 part; σ_max: 205 MPa

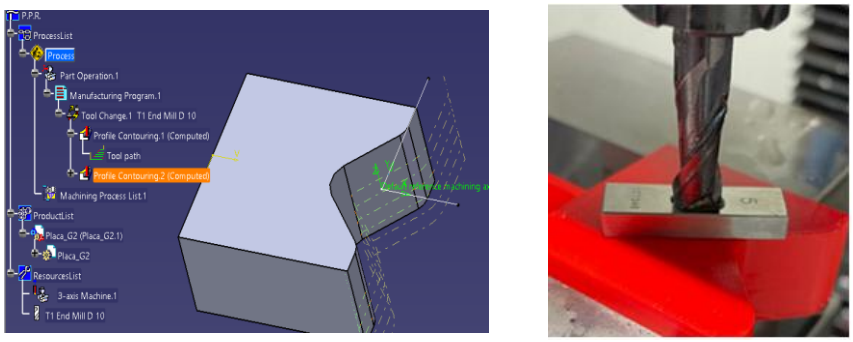
• Maximum stress values in the active elements of the mold are reached in the connected areas of the active surfaces of the punch and the active plate, respectively, of 41 MPa for the active elements made of PLA and 33.3 MPa for the active elements made of PETG (see also Fig. 8.18).

8.4. Testing a PLA MIV mold

For the experimental research of a PLA MIV mold, the structural model developed for cold V-bending processing of Pg2 parts was selected (see Fig. 8.2 – c).

Elements regarding the manufacturing of the punch and active plate of the PLA MIV mold
The punch and active plate of the MIV PLA mold, with the dimensions in Fig. 8.2 - c, were manufactured by 3D printing and milling of the active surfaces, under specific working conditions similar to those presented in § 5.1.1 d - g, 5.4.1, 6.3.1, 7.2, with the following mentions:

elements regarding the generation of the CNC Program Milling active plate and the zero adjustment of the processing technological system are presented in Fig. 8.22; the total prescribed allowance for the active surfaces, with the value of 0.9 mm, was processed by CNC roughing and finishing milling (0.2 mm), with the T01 cylindrical end mill, the main cutting depth a_p of 4 mm,



a) b)

Fig. 8.22. CNC program generation Active plate milling in Catia V5R21: a) CNC simulation; b) zero adjustment on the technological system in the Z direction

feed per tooth of f_z 0.0331 mm/tooth and cutting speed $V_c$of 87.03 m/min (speed n_c of 3463 rpm, feed speed F of 229 mm/min).

Experimental determination of the cold V-bending force of some Pg2 parts

The cold V-bending force of Pg2 parts, with width B of 15 and 20 mm, was determined experimentally on the INSTRON 8872 testing machine (see § 8.2). The bending force was measured during the machining process at a loading rate of 5 mm/min.

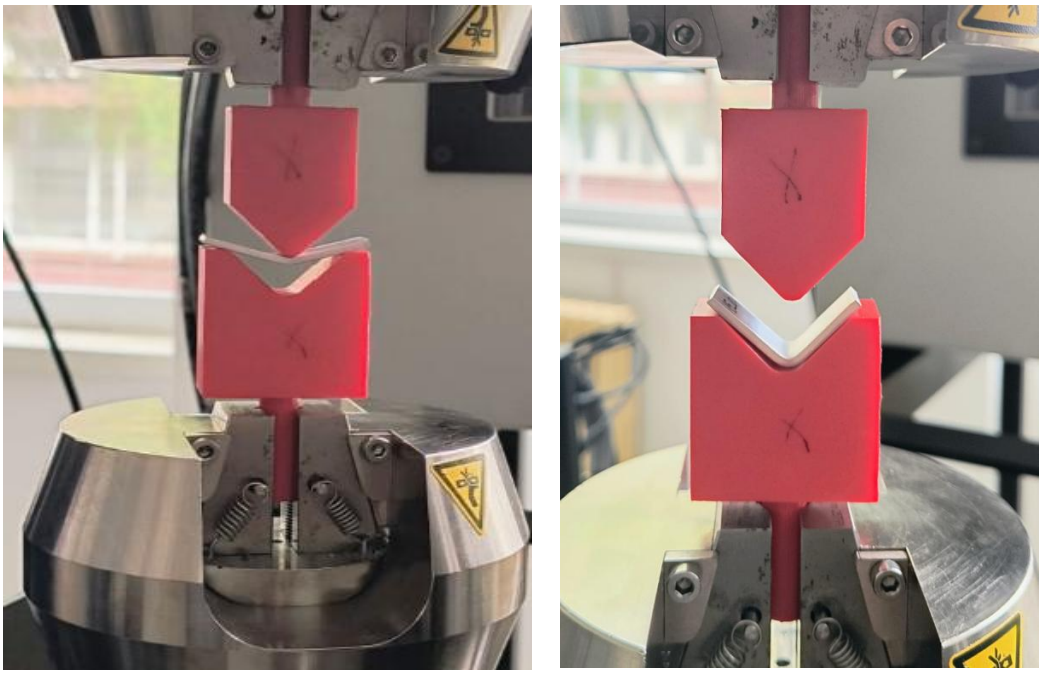


Fig. 8.23. Experimental determination of the cold V-bending force of some Pg2 parts

The results for Pg2 parts with width B of 15 mm and 20 mm are presented in Fig. 8.24. It is noted that, in order to avoid critical stresses on the punch and the active plate, loading was carried out up to approximately 90% of the full stroke, a position in which the bending force increases significantly.

Chapter 9. Final conclusions and main contributions to the modeling and precision evaluation of elements and molds made of thermoplastic materials produced by additive manufacturing and cutting

(1) From the analysis of the current state of the art regarding the manufacturing and precision of thermoplastic elements and molds produced by additive manufacturing and machining, important conclusions were drawn, which are presented in Chapter 3.

(2) In relation to the data and conclusions drawn from the analysis of the current state of the art regarding the manufacturing and precision of thermoplastic elements and molds produced by additive manufacturing and machining, the research and development directions as presented in § 4.1 were considered to be promising.

(3) Considering the data and conclusions drawn from the analysis of the current state, as well as the research and development directions regarding the development of thermoplastic elements and molds, the main objective of the advanced doctoral research and development activity (see also § 4.2) was determined as: **modeling and precision evaluation of elements and molds produced by additive manufacturing and cutting**.

(4) The relevant conclusions regarding the doctoral research and development activity to achieve the main objective, in relation to the methodological reference elements (see § 4.3), are as follows.

○ Considering the shape and relative position of the surfaces in the structure of some 3D printed mold components made of PLA or PETG, as well as the different milling processing schemes, the PLA/ PETG - Frontal milling, PLA/ PETG - Cylindrical milling and PLA/ PETG - Cylindrical-frontal milling research programs were structured: 3D printing of a series of parts from PLA/ PETG; for the printed parts, CNC milling processing of flat surfaces of different positions, namely, *horizontal* - by frontal milling, *vertical* - by cylindrical milling, *inclined* - by cylindrical-frontal milling; modeling and analysis of the roughness parameters Ra, Rz, as well as the dimensional accuracy related to some flat surfaces of the printed parts and, accordingly, the *horizontal, vertical, inclined* flat surfaces processed by CNC milling. (see § 5.1.1. 6.1.1).

○ The types of PLA and PETG materials, parts and surfaces, CNC milling processing schemes, elements of 3D printing and CNC machining technological processes and systems were determined.

○ Evaluation of the roughness and dimensional accuracy of 3D printed parts made of PLA/PETG shows that for horizontal surfaces, the roughness parameter Ra* has effective values in the roughness classes N 8 – 9/ N 9 - 10, and for vertical and inclined surfaces - in the roughness classes N10 – 11; dimension C* has effective values in the tolerance class IT12.

○ Within the PLA/PETG research programs - Face/cylindrical/cylindrical-face milling, regression functions for roughness and dimension of machined surfaces were configured where, as appropriate: the dependent variables are the roughness parameters Ra and Rz, as well as the distance C between two parallel machined surfaces; the independent variables are the feed per tooth and the cutting speed or the speed and feed rate or the adjustment feed; the variation ranges of the independent variables were determined based on preliminary tests; the analytical models are of the power type (see § 5.1.3, 6.1.3).

○ Within the research on the development of technological models from PLA for the manufacture of silicone molds applied to the casting of polyurethane resin parts: two technological models MT1 and MT2 were defined that participate in the manufacture, by casting, of silicone molds, MS1 and, respectively, MS2; the MS1 and MS2 molds were used in the manufacture, by casting, of the products P1 and, respectively, P2.

The research aims to evaluate the influence of the roughness and dimensional accuracy of the MT1 and MT2 models in the manufacture of the silicone molds MS1 and, respectively, MS2, based on the analysis of the characteristics of the products P1 and, respectively, P2 made by casting in the silicone molds considered (see § 7.1).

○ In order to apply the finite element analysis, the effective tensile properties of the PLA, PETG and Al materials of the component elements of the structural model were determined, under the conditions regulated by ISO 527.

(5) In achieving the main objective of the doctoral research and development activity, this doctoral thesis brings a series of contributions, the most important of which are as follows.

• Structured study of the current state of research - development and applications regarding the manufacture and precision of elements and molds from thermoplastic materials produced by additive manufacturing and machining.

• Development and scientific implementation of complex theoretical and experimental research on the modeling and evaluation of the accuracy of PLA and PETG elements and molds produced by additive manufacturing and CNC milling, respectively, the initiation, configuration and detailed preparation of operational research programs, the establishment and adjustment of technological elements and systems for 3D printing, CNC milling processing, assisted tensile stress, control, as well as the performance of experiments, analysis and interpretation of results.

• Modeling and determination of roughness and dimension functions, as multivariable regression functions, associated with certain surfaces in the composition of PLA and PETG elements, processed by CNC frontal, cylindrical and cylindrical-frontal milling.

• Development and manufacturing by 3D printing and milling of technological models from PLA, their use in the manufacture of silicone molds, with the evaluation of the influence of the geometric accuracy of technological models on the characteristics of polyurethane resin parts made by casting in the considered molds.

• Initiating and conducting research on finite element analysis, manufacturing and testing of PLA and PETG molds for precision cold bending/calibration.

* * *

This doctoral thesis, through its issues, approach and results, develops the modeling and precision evaluation of PLA and PETG elements and molds produced by additive manufacturing and CNC milling.

The scientific importance of this doctoral thesis is supported by the contributions made to the structured study of the current state of research – development, modeling and determination of roughness and dimension functions as multivariable regression functions, development and manufacturing of technological models from PLA and their use in the manufacture of silicone molds, initiation and implementation of research on finite element analysis, manufacturing and testing of PLA and PETG molds for precision cold bending/calibration.

The practical importance of this doctoral thesis lies in the fact that the models, systems and data as well as the research results represent a useful support system for students, teachers, organizations, specialists and industrial companies.

The issue of developing products from thermoplastic materials through assisted design, additive manufacturing and CNC machining, as potential future directions, requires continuous, complex and deep research and development activity.